Klepatzki, J. P. and S. M. Milrad, 2026: Multiscale analysis of Dixie Alley tornado and null events. *Electronic J. Severe Storms Meteor.*, **21** (1), 1–35.

Electronic Journal of
SEVERE STORMS METEOROLOGY

Multiscale Analysis of Dixie Alley Tornado and Null Events

JONATHON P. KLEPATZKI
Las Vegas, Nevada

SHAWN M. MILRAD
Embry-Riddle Aeronautical University, Daytona Beach, Florida

(Submitted 13 May 2024; in final form 20 January 2026)

ABSTRACT

Some of the most destructive tornadoes throughout history have occurred in what is known as Dixie Alley within the Southeast U.S. Previous studies for Florida defined a tornado event as ≥4 tornadoes within a 24-h period during December–May (avoiding tropical cyclone related events), while a null event was defined as a period when the NOAA Storm Prediction Center had tornado outlook probabilities ≥5% over any part of the respective study area, but <4 tornadoes occurred in 24 h. This study presents a multiscale composite analysis (2002–2019) of 33 Alabama tornado and 65 null events; 46 Mississippi tornado and 92 null events; 24 Louisiana tornado and 98 null events; and 21 Georgia tornado and 32 null events. Like the Florida cases, tornado events were primarily experienced across the northern and central parts of each state. Using archived frontal analyses from the NOAA Weather Prediction Center, tornado events were associated with stationary boundaries more than any other synoptic or mesoscale feature (e.g., cold front; warm front). Tornado events also occurred more frequently during La Niña and a positive Arctic Oscillation (AO) pattern. A composite synoptic analysis showed jet-streak divergence, amplified anomalous midtropospheric troughing, and large positive precipitable water and potential temperature anomalies from Louisiana through Georgia during tornado events. However, Louisiana tornado events featured more 850-hPa southerly winds compared to the classic southwesterly winds seen across its Dixie Alley counterparts.

1. Introduction

Tornado events across the southeastern U.S. (hereafter Southeast), also known as "Dixie Alley" (DA) (Schaefer et al. 1980; Gagan et al. 2010; Dixon et al. 2011), are dangerous due to the proximity of socially vulnerable population areas. For example, using the Centers for Disease Control and Prevention (CDC) Social Vulnerability Index (SVI), select counties that have the average highest mobile-home density (≥0.7, no higher than 1.0) across DA also have a high level of vulnerability (Fig. 1). The term DA originated from former National Severe Storms Forecast Center (NSSFC) Director Allen Pearson after monitoring the Mississippi (MS) Delta outbreak of 21 February 1971 (Gagan et al. 2010). This area refers to the states of Louisiana (LA), Arkansas (AR), Mississippi (MS), Alabama (AL), Georgia (GA), and parts of Tennessee (TN) (Gagan et al. 2010).

Gagan et al. (2010) would go on to note that DA has been used by professionals who lived in these areas. Other papers noted this area has a high frequency of tornado activity and long-track violent tornadoes like those across "Tornado Alley" (Brooks et al. 2003; Broyles and Crosbie 2004). More recent studies (Gagan et al. 2010; Dixon et al. 2011; Anderson-Frey et al. 2019) found that DA tornadoes occurred on average during the afternoon. However, some studies (Hagemeyer and Schmocker 1991; Hagemeyer 1997; Anderson-Frey et al. 2016, 2019; Bunker et al. 2019; Klepatzki and Milrad 2020) found that tornadoes across parts of the Southeast (e.g., Florida) can develop at night. This was also echoed by Kelly et al. (1978), who found a daytime maximum in the distribution of tornadoes, particularly in the late afternoon with minimum tornado counts occurring during the early morning.

Corresponding author address: Jonathon P. Klepatzki, E-mail: klepatzkijonathon@yahoo.com

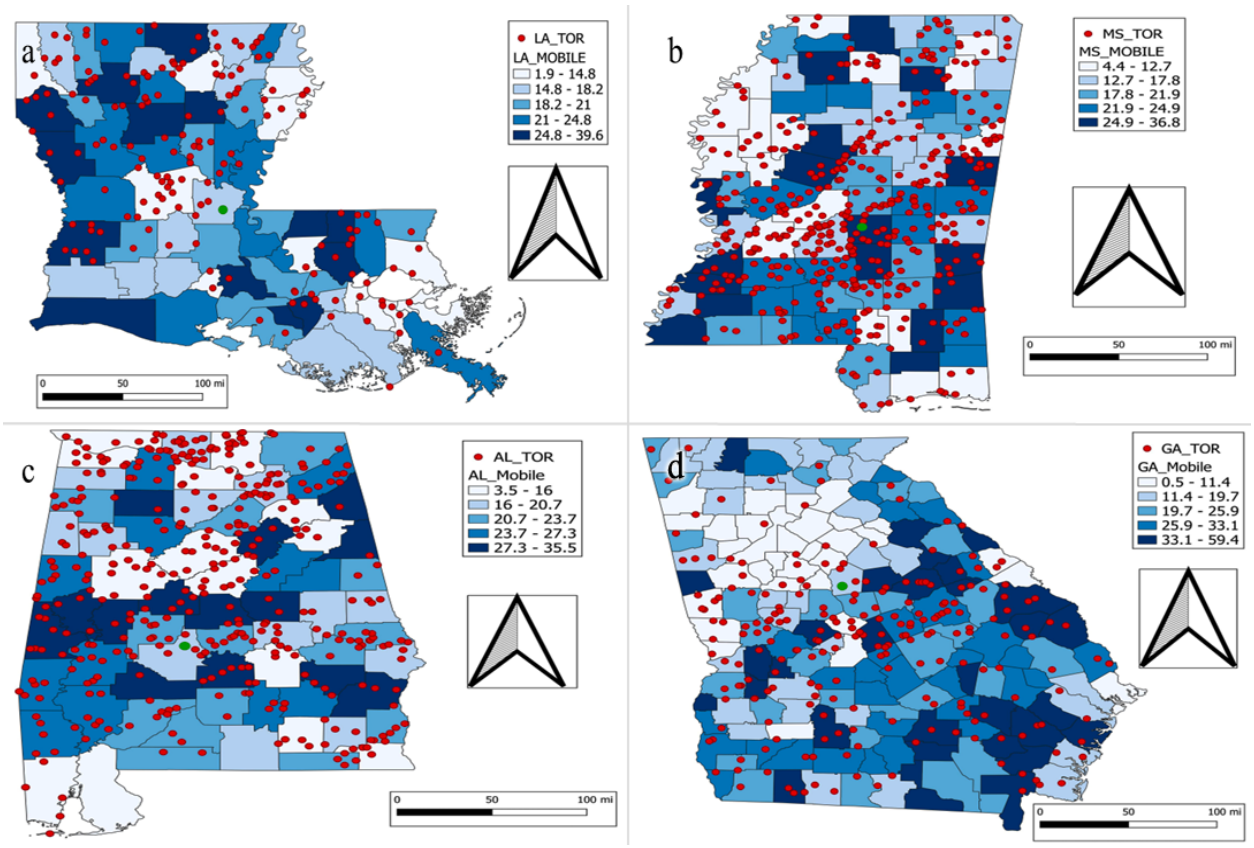

Figure 1: Locations and spatial extent of cool-season tornadoes (2002–2019; red dots) and the mean tornado location in each state (green dots) for: a) Louisiana (21 events); b) Mississippi (46 events); c) Alabama (33 events); and d) Georgia (24 events). In all panels, the mobile-home percentage of each state is shaded.

Synoptic-scale dynamics are also important. Means et al. (1955) showed that squall lines were associated with stationary boundaries across the Central U.S. They also noted that squall lines occurred in the right-front quadrant of a jet streak along an east–west-oriented jet stream. This matched well with the dynamic features that Megnia et al. (2019) found in composites of the 2 April 2017 event in LA. Such events (e.g., 26 and 27 April 2011, 24 April 2015) led to numerous tornadoes.

Other studies (Lee et al. 2016; Molina et al. 2016, 2018; Molina and Allen 2019; Brown and Nowotarski 2020) investigated the relationship between El Nino-Southern Oscillation (ENSO) and the moisture sources that impact tornado events. Molina et al. (2016, 2018) specifically noted that sea surface temperatures in the Gulf of Mexico (GOM) can remain cooler due to increased amounts of cloud cover, suggesting both an independent teleconnection and seasonal predictability of moisture transport across the Southeast. Gaffin and Parker (2006) previously noted that tornadoes in the Southeast were favored by 500-hPa southwest flow, and were primarily related to surface boundaries rather than to large-scale terrain features.

The primary objective of this study is to investigate the multiscale characteristics associated with DA tornado events during the cool season, outside the Atlantic and GOM tropical cyclone (TC) season (December–May). Klepatzki and Milrad (2020) performed similar analyses for Florida, but this study extends it to other states in the Southeast.

A key similarity between DA and Florida is the high-shear/low-CAPE (HSLC) environments (King et al. 2003; Sherburn and Parker 2014; Cohen et al. 2015, 2017; Sherburn et al. 2016; Anderson-Frey et al. 2016, 2019; Klepatzki and Milrad 2020). While much of Florida is near sea level and surrounded by water, the same cannot be said for large portions of the greater Southeast. Therefore, the environmental characteristics associated with tornado events may differ between Florida and elsewhere in the region.

This paper is organized as follows: section 2 details the data and methods, section 3 details teleconnection and composite synoptic, and section 4 presents overall conclusions and suggestions for future studies.

2. Data and methodology

Klepatzki and Milrad (2020) defined a tornado (TOR) event as ≥4 tornadoes occurring in 24 h. While DA TOR events are larger in rating, frequency, and path lengths and widths (Brooks et al. 2003; Broyles and Crosbie 2004), using the same methodology above will provide scientific consistency. The consistency later could build a uniform definition of tornado events, despite areas within the Southeast having different levels of tornado activity. In turn, this would allow for a large case repository to perform synoptic composites across and/or within the region.

We found 24, 46, 33, and 21 TOR events across Louisiana, Mississippi, Alabama, and Georgia, respectively, for 2002–2019. Each of these occurred when an enhanced risk or greater was issued by the NOAA Storm Prediction Center (SPC) (see Tables A1; A3; A5; A7) outlook since 2014, when enhanced risks were implemented, and moderate risk or greater from 2002–2013. This was done by retrieving tornado reports from the 2002–2019 period corresponding to the SPC outlook archive and the NULL case study period of Klepatzki and Milrad (2020).

We also investigated the occurrence of surface boundaries using the NOAA Weather Prediction Center's (WPC) surface analysis archive between 12 and 00 UTC (Tables A13 and A14). This revealed that stationary boundaries occurred in 38–44% and 29–37% of our TOR and NULL cases, respectively.

To analyze synoptic-scale environmental parameters, we used the North American Regional Reanalysis (NARR, Mesinger et al. 2006). The NARR has a 32-km horizontal grid spacing, 3-h temporal resolution, and is available from 1979–present. Gensini and Ashley (2011) previously showed that NARR convective environments generally corresponded to severe storm reports. Like Klepatzki and Milrad (2020), we used SPC storm reports to map the spatial extent of all tornado events and produced composite charts for each through the Quantum Geographic Information System (QGIS) (Figs. 1a–1d).

Klepatzki and Milrad (2020) also defined a NULL event as one in which the 0600 UTC SPC Day 1 tornado outlook featured probabilities ≥5% over any part of each state, but <4 tornadoes in 24 h were observed. Event duration was defined as from the first hail/wind report to the last. We found 98, 92, 65, and 32 NULL events for Louisiana, Mississippi, Alabama, and Georgia, respectively (Tables A2; A4; A6; A8).

Null events were not plotted, but by using SPC hail and wind reports, we determined that the majority occurred in the northern portions of each state, like in Florida (Klepatzki and Milrad 2020). The geographic distribution of tornado events revealed a larger percentage of mobile homes in those areas (Figs. 1a–d), echoed by Klepatzki and Milrad (2020) and Anderson-Frey et al. (2019).

We also performed a statistical analysis on the spatial extent of tornado events using QGIS. This was done using the starting latitude and longitude (i.e., slat and slon) of all tornado reports. We found the geographic center of tornado activity in each state occurred at: 31.49°N, –92.02°W (LA); 32.60°N, –89.55°W (MS); 33.19°N, –86.72°W (AL); and 32.55°N, –83.41°W (GA). The third quartiles (northern reports) were located at: 32.37°N, –91.23°W (LA); 33.32°N, –89.41°W (MS); 34.25°N, –86.14°W (AL); and 33.12°N –82.60°W (GA), while the first quartile (southern reports) were at: 30.69°N, –92.78°W (LA); 31.82°N, –90.09°W (MS); 32.37°N, –87.48°W (AL); and 31.91°N, –84.27°W (GA). These revealed that tornado events favored the northern and central portions of each state.

The polar front, subtropical, and low-level jets (i.e., PFJ, STJ, LLJ) are important features to consider during tornado events. Kis and Straka (2010) defined the LLJ as a relatively narrow band of wind that is stronger than the 850-hPa geostrophic flow. Weaver et al. (2012) found that over a 32-y period, LLJs existed in three distinct areas: the Southeast and the northern and southern Great Plains. LLJs coupled to an upper-tropospheric jet streak have also been studied (Uccellini and Johnson 1979; Klepatzki and Milrad 2020). The coupling of the PFJ and LLJ allows an increase in vertical wind shear. To promote the release of θe and precipitable water for severe convection, quasistationary boundaries are also often present (Tables A13, A14). The ascent and moisture ingredients are further explored in our composite synoptic analysis in section 3.

Weaver et al. (2012) noted substantial moisture flux from the enhanced convergence associated with the northerly LLJ over the Plains. In addition, LLJs were more susceptible to the variability of the Atlantic Multidecadal Oscillation (AMO) specifically during the months of April and May. This ultimately affects the heat and moisture distribution and is discussed further in section 3.

Moisture is a key ingredient for tornado events (e.g., Thompson et al. 2013; Klepatzki and Milrad 2020), both in terms of dewpoints and precipitable water. Precipitable water (W) is defined as

$$W = \frac{1}{\rho g}\int_{P1}^{P2} q dp, \quad (1)$$

where g is the gravitational acceleration, ρ is the density of liquid water, q is specific humidity, and dp is the differential representing the change in pressure between two pressure levels P. Larger W anomalies equate to high specific humidity in the troposphere, which is concentrated in the lower troposphere and favorable for severe convection. This will be discussed in section 3.

3. Synoptic-scale analysis

a. Teleconnections

Some studies (e.g., Brown and Nowotarski 2020; Klepatzki and Milrad 2020) have evaluated ENSO and AO during Southeast tornado events. Brown and Nowotarski (2020) noted the AO index was ≥2 during tornado events with null cases varying between –1 and 1 over 60 days. Klepatzki and Milrad (2020) observed similar results across Florida. Klepatzki and Milrad (2020) chose this to measure AO strength during tornado events, as AO exhibits more short-term variability than ENSO.

Following the methodology of Klepatzki and Milrad (2020), we tabulated both the NOAA Multivariate ENSO Index (MEI; Wolter and Timlin 2011) and the Climate Prediction Center (CPC) Oceanic Nino Index (ONI). CPC and previous studies defined ONI values ≥0.5 as El Niño; values of ≤ –0.5 indicate La Niña (see Tables A9, A10, A11 and A12). To retrieve the daily AO data, we used the daily data from the CPC archive.

To be consistent with the CPC definitions and Klepatzki and Milrad (2020), orange and blue shading is used for AO index values greater or less than 0.5, respectively. The positive (negative) AO may indicate that the jet stream patterns were zonal (meridional). These results corresponded to past studies (e.g., Means et al. 1955; Megnia et al. 2019) and our synoptic composites in sections 3b–3e.

We found DA TOR events favored La Niña and a positive AO (Tables A9; A10; and A11) except for a negative AO across GA cases (Table A12). This finding differed from previous studies (e.g., Hagemeyer 1997, 2010; Adams-Fought 2010; Molina et al. 2018; Brown and Nowotarski 2020; Klepatzki and Milrad 2020). Older studies (Lloyd 1942; Showalter and Fulks 1942; Crawford 1950; Fulks 1951) found that favorable conditions for tornadoes in GA were different compared to locations farther west, particularly with respect to squall-line formation. Therefore, tornado events within states near the Atlantic Coast plausibly are associated with different teleconnection phases than locations farther west.

Of the total number of positive and negative ENSO cases during our tornado events, we found:

- LA: Six occurred during El Niño and three during La Niña.
- MS: 12 occurred during El Niño and 13 during La Niña.
- AL: Eight occurred during El Niño and nine during La Niña.
- GA: Three occurred during El Niño and nine during La Niña.

For El Niño cases, the mean ONI was:

- LA: +1.23
- MS: +1.25
- AL: +1.20
- GA: +1.36

For La Niña cases, the mean ONI was:

- LA: –0.70
- MS: –0.81
- AL: –0.82
- GA: –0.91

For AO, we found:

- LA: 10 (+AO) and nine (–AO) TOR events
- MS: 22 (+AO) and 17 (–AO) TOR events
- AL: 18 (+AO) and 10 (–AO) TOR events
- GA: Seven (+AO) and 10 (–AO) TOR events

For AO, the positive/negative mean tornado event values were:

- LA: +1.43/–1.30
- MS: +1.68/–1.61
- AL: +1.31/ –1.20
- GA: +1.28/–1.11

Compared to the findings of Klepatzki and Milrad (2020), FL (–0.9) and GA (–0.91) exhibited similar results for La Niña; however, they were different in terms of El Niño. Klepatzki and Milrad (2020) found FL cases had a mean ONI of +2.17, which is substantially stronger than all the average El Niño events across DA (+1.26). GA had an average El Niño event ONI of +1.36, a +0.81 difference from FL. The difference in El Niño event ONIs suggests weaker enhancement of LLJs across DA in comparison to tornado events across FL. The weaker enhancement of LLJs was identified in a study that concluded the frequency and location of significant tornadoes vary by ENSO phase and strength (Brown et al. 2020). Another study showed similar results where the Caribbean low-level jet (CLLJ) was weaker during warm anomalies in the Pacific, reducing DA precipitation (Wang 2007).

For the NULL events, we found the following number of cases during El Niño/La Niña phases:

- LA: 32/25
- MS: 21/20
- AL: 9/18
- GA: 7/8

The mean ONIs were:

- LA: +1.14/–0.83
- MS: +1.04/–0.75
- AL: +1.34/–0.77
- GA: +1.05/–0.76

We found the following numbers of +AO/–AO NULL events:

- LA: 35/36
- MS: 41/28
- AL: 23/22
- GA: 18/8

The mean values of the AO index for +AO/–AO events were:

- LA: +1.53/–1.82
- MS: +1.41/–1.44
- AL: +1.84/–1.49
- GA: +1.62/–1.24

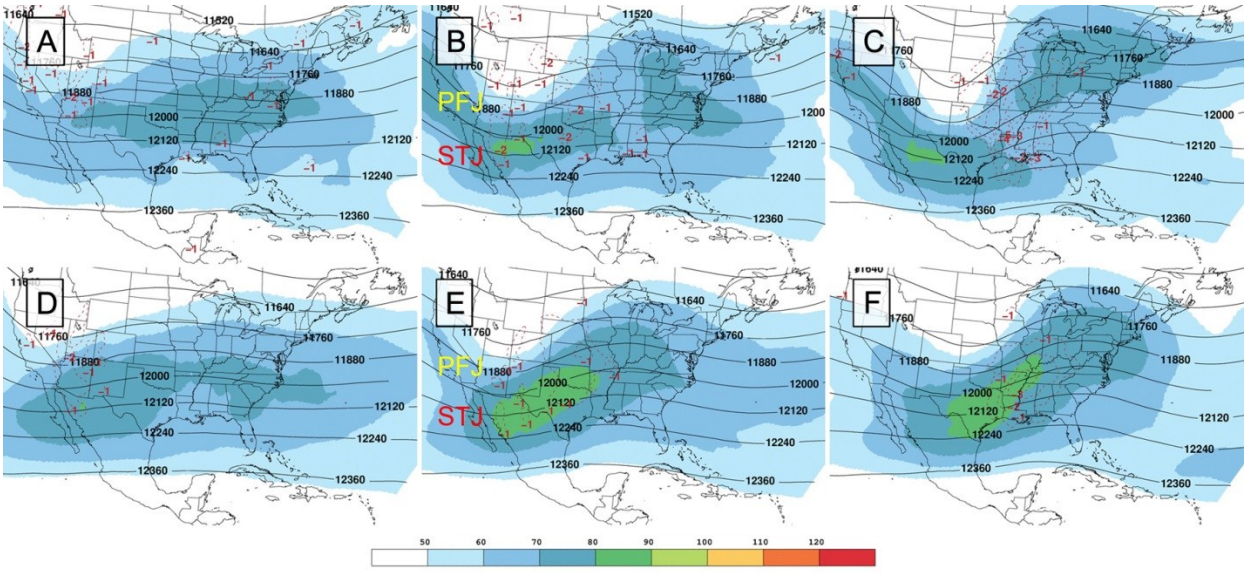

Figure 2: NARR composites of LA (a–c) tornado (TOR) and (d–f) null (NULL) events. Plotted are mean 200-hPa windspeed (kt, shaded; 1 kt = 0.51 m s^{-1}), geopotential height (m, solid black contours), and 700–400-hPa layer-averaged vertical velocity magnitude ω (x 10^{-2} Pa s^{-1}, negative values plotted with red dashed contours) at (a,d) –48, (b,e) –24, and (c,f) 00 h. The origins of the polar front jet (PFJ) and subtropical jet (STJ) are marked on (b) and (e). *Click image to enlarge.*

Like Klepatzki and Milrad (2020), the intent is not to make broad, statistically significant conclusions. However, to improve the understanding of synoptic composite structures in the context of the AO evolution, a more in-depth comparison is needed. This will be investigated in sections 3(b–e). This analysis also provides an idea of differences over a wider spatial area.

Numerous TOR events also developed along stationary boundaries over more than one state and ≥2 days (see Table A15). This phenomenon occurred in all months, although it was most common in March and April (≈11 events). In fact, 32% of our TOR cases in MS and AL were associated with stationary boundaries (Table A15).

b. Large-scale composites: LA

Compared to the rest of DA, LA has the highest number of NULL events and second fewest TOR events (Tables A5 and A6). Previous studies (Galway et al. 1981; Anderson-Frey et al. 2016, 2019; Megnia et al. 2019; Bryant et al. 2022) have investigated the synoptic and mesoscale conditions of these events. Galway et al. (1981) found that an amplified anomalous trough extended from CO through NM, with a mean 40-kt LLJ near the Texas/LA border. Galway's findings were similar to the results of this paper at the 200, 500 and 850-hPa levels (Figs. 2–5). However, Galway et al. (1981) were limited to 23 TOR and 6 NULL events over a 30-y period compared to the results of this paper over an 18-y span (24 TOR events). Megnia et al. (2019) later conducted a rapid refresh (RAP) model analysis of one of the worst TOR events in LA (2 April 2017). They noted an amplified anomalous trough that was slightly eastward in comparison to Galway et al. (1981). Our AO analysis revealed that the mean TOR (+0.05) and NULL (–0.03) events were AO-neutral across LA over a three-day period. This corresponds to amplifying and increasingly meridional 200- and 500-hPa patterns between –48 h and –24 h (Figs. 2a,b; 3a,b), followed by less 200-hPa amplification between –24 and 00 h (Fig. 2c).

Jet-stream locations and tornado occurrences have been studied over many years (e.g., Beebe and Bates 1955; Skaggs 1967; Clark et al. 2009; Klepatzki and Milrad 2020). This also includes tornadoes that form within or along QLCS boundaries (e.g., Williams et al. 2018). For example, Williams et al. (2018) noted that on 20 February 2017, strong 300-hPa south-southwesterly winds up to 90 kt were surrounded by a ≥100-kt (≈50-m s^{-1}) jet streak and a northeastward-moving trough between New Mexico (NM) and Texas (TX). Strong differential positive vorticity advection (DPVA) was associated with widespread ascent across TX which led to a QLCS TOR event (nine reported tornadoes). This is important, as we will see similar synoptic structures across DA later in this manuscript.

We extended the composite period examined in Klepatzki and Milrad (2020) back to –48 h and increased the height of the layer from 250-hPa to 200-hPa to emphasize the role of the STJ. Figure 2 shows NARR 200-hPa wind speed and geopotential height composites at –48, –24, and 00 h; 700–400-hPa layer-average ω is also plotted to analyze large-scale vertical motion.

Investigation of the 200-hPa composites across LA revealed multiple differences in jet streaks compared to MS, AL, and GA (sections 3c–e). The area of expansion that extends (i.e., north–south) into the Gulf suggests more than one jet contributes to TOR events. Unlike the PFJ and STJ across these states, this region is more zonal for NULL events, while the opposite is true during TOR events (Figs. 2b,c,e,f). Furthermore, the right exit and left entrance of the PFJ (Figs. 2b,c) couple over northern LA. The biggest difference is the intensity of the jet streak over the 48-h period. The PFJ across LA exhibited the weakest (similar) intensity on average during TOR (NULL) events. For example, at peak intensity during TOR events, MS, AL, and GA all exhibited 90–100 kt (45–50 m s^{-1}) compared to the80–90 kt (40–45 m s^{-1}) seen over LA over the 48-h period. This corresponds to lower (higher) amounts of shear and larger ascent, with potential QLCS development, matching the results found by Klepatzki and Milrad (2020).

At 00 h (Fig. 2f), the TOR (-5×10^{-2} Pa s^{-1}) and NULL events (-3×10^{-2} Pa s^{-1}) have similar ω. These higher and lower values of omega correlated well to the locations where most tornado reports occur (see section 2) and are like the Florida results of Klepatzki and Milrad (2020). Another similarity is the influences from the PFJ and STJ between –24 h (Fig. 2b) and 00 h (Fig. 2c), with evidence indicating these features maintaining the trough during its life cycle.

Following Klepatzki and Milrad (2020), 500-hPa height patterns are an important forecast tool for severe weather events. Figure 3 shows monthly-weighted anomalies and composite means. The 500-hPa composites revealed zonal

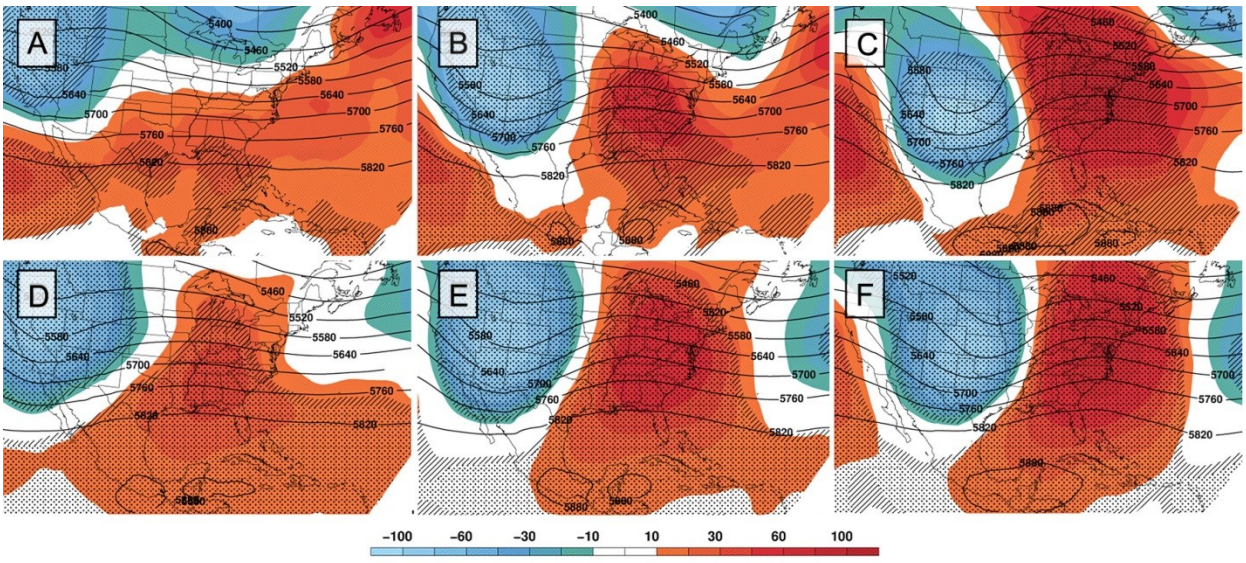

Figure 3: For LA (a–c) TOR and (d–f) NULL events: NARR 500-hPa geopotential height monthly-weighted composite anomalies (m, shaded) and composite mean (m, solid black contours) at (a,d) –48, (b,e) –24, and (c,f) 00 h. Gridpoints with statistically significant anomalies at the 95% and 99% confidence intervals according to the Student's t-test are hatched and dotted, respectively. *Click image to enlarge.*

flow across DA prior to TOR events at –48 h (Fig. 3a). This is also evident with a more west–east orientation pattern across the southern and southeastern regions of the continental U.S., but later changes as the pattern becomes more amplified over eastern CO and western TX (Fig. 3c).

NULL events, on the other hand, suggest a more positively-tilted trough located farther east than TOR cases over the 48-h lifecycle (Figs. 3d–f). In association with a stronger subtropical ridge (STR) in the Western Caribbean Region (WCR), this would increase θ_e and W composite anomalies earlier but remain weaker in comparison to its TOR event counterparts (Figs. 4 and 5).

To help investigate the LLJ structures, Fig. 4 shows the 850-hPa θ_e composite means and anomalies, as well as 850-hPa mean winds from –48 to 00 h. Figure 4a shows a relatively weak θ_e anomaly (2–4 K) associated with a westerly wind field. However, θ_e increases (8–12 K) between Fig. 4b and 4c during TOR events. NULL cases show similar results with the biggest difference occurring –48 h prior to the event (Fig. 4d). The TOR and NULL composites also suggest large θ_e and W (Fig. 5) originate in the Yucatan Peninsula. Molina and Allen (2019) echoed this, finding an average of 40–60% (TOR) and 15–45% (NULL) cases have high-θ_e air origins near the Yucatan during the cool-season. Evidence of this can be seen in Figs. 4 and 5 from –48 h to 00 h.

c. Large-scale composites: MS

Due to their proximity, one may assume similarities between LA and MS. Figure 6 shows MS TOR cases had 200-hPa wind speed magnitudes of 80–110 kt (40–55 m s^{-1}) as the pattern evolved over 48 h, which is a 20 kt difference (10 m s^{-1}) from LA TOR cases (Fig. 2). MS TOR cases were also influenced by a more amplified anomalous trough, while a less amplified trough existed during LA cases (Figs. 2,3,6,7). Furthermore, MS TOR cases (Figs. 6a–c; 7a–c) exhibited a shortwave over western TX and a slight negatively-tilted trough in eastern TX compared to a single longwave trough during LA TOR cases.

Throughout the 48-h lifecycle, both LA and MS cases showed similar ω values (-2×10^{-2} Pa s^{-1}) across their respective states. Maximum ω values during MS TOR cases on the other hand were slightly stronger (-6×10^{-2} Pa s^{-1}). However, these values were located over the northern Gulf, in comparison to those over land in LA (Fig. 6).

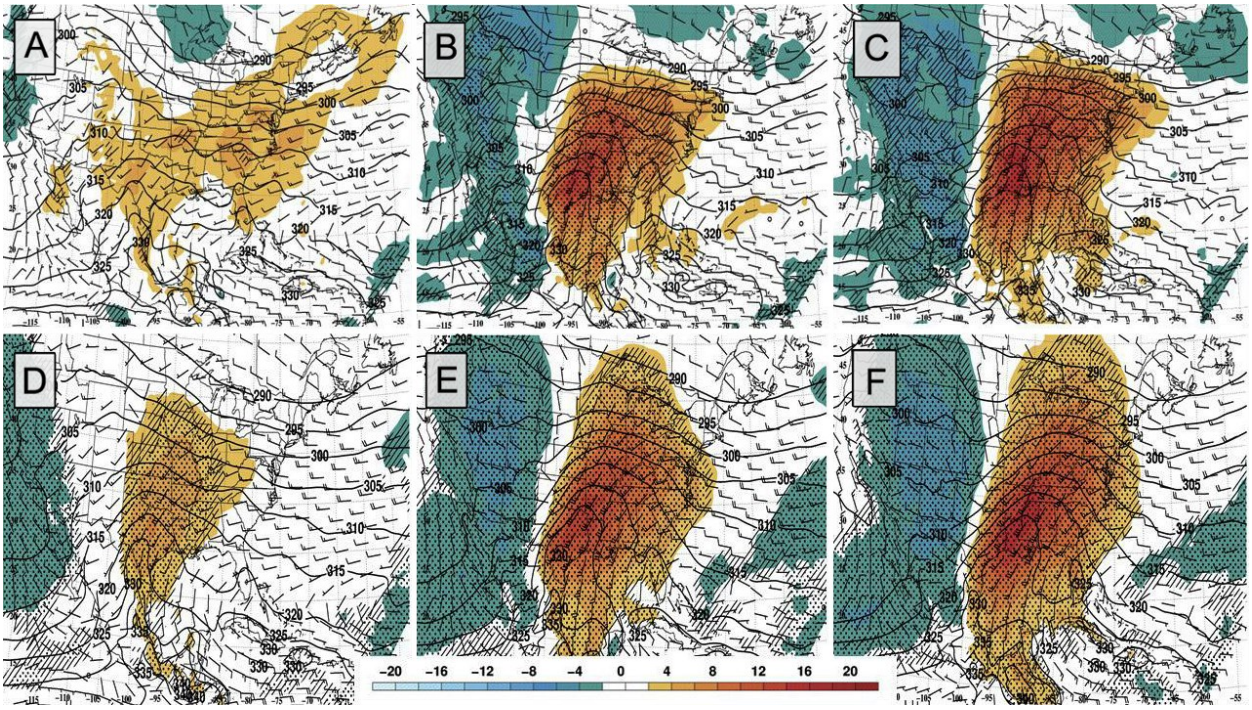

Figure 4: For LA (a–c) TOR and (d–f) NULL events, NARR 850-hPa θ_e monthly-weighted composite anomalies (K, shaded) and means (K, solid black contours), and 850-hPa composite mean wind (kt, barbs) at a and d) –48, b and e) –24, and c and f) 00 h. *Click image to enlarge.*

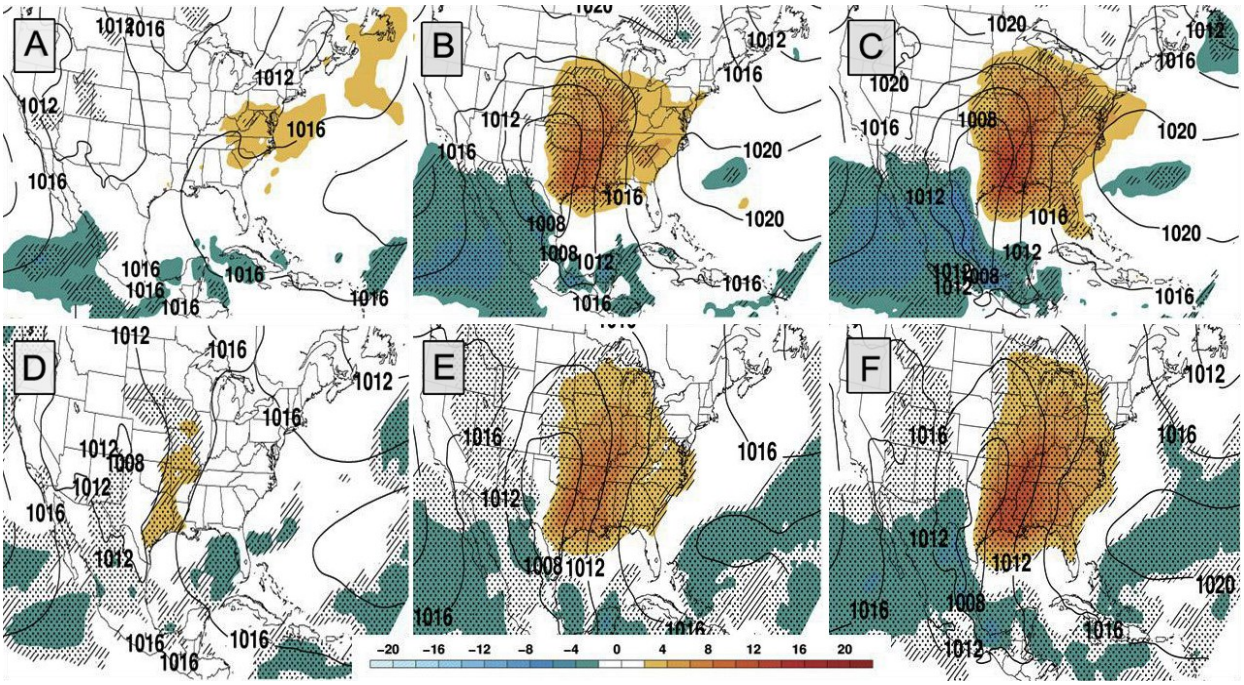

Figure 5: For LA (a–c) TOR and (d–f) NULL events, NARR monthly-weighted composite anomalies of precipitable water (mm, shaded) and composite mean MSLP (hPa, solid black contours) at (a,d) –48, (b,e) –24, and (c,f) 00 h. Gridpoints with statistically significant anomalies at the 95% and 99% confidence intervals according to the Student's t-test are hatched and dotted, respectively. *Click image to enlarge.*

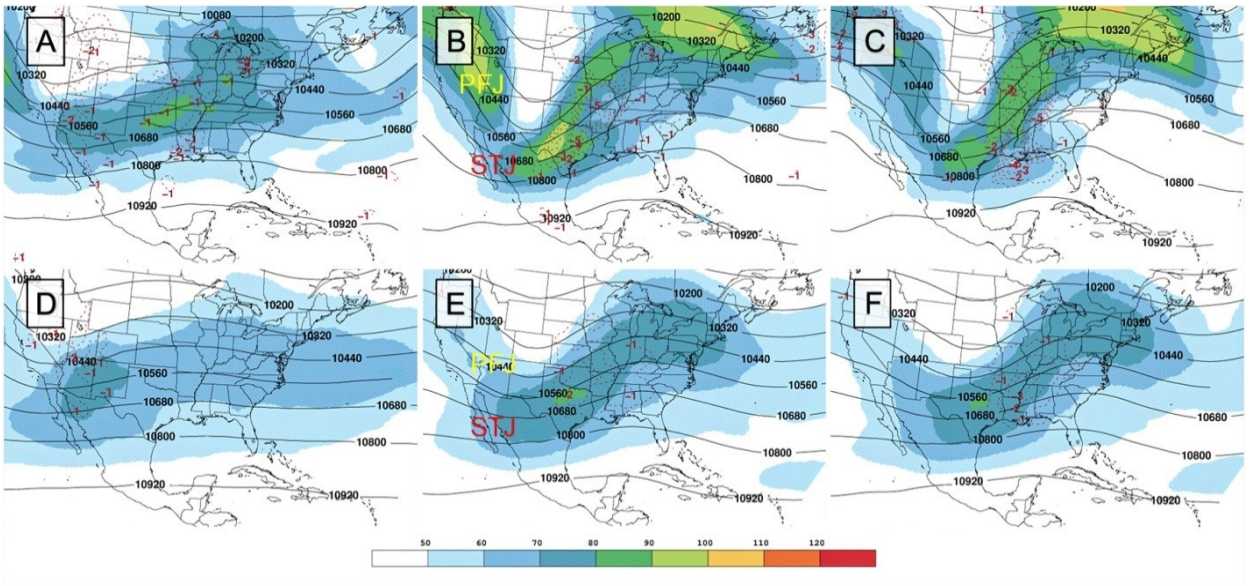

Figure 6: As in Fig. 2, but for MS events. *Click image to enlarge.*

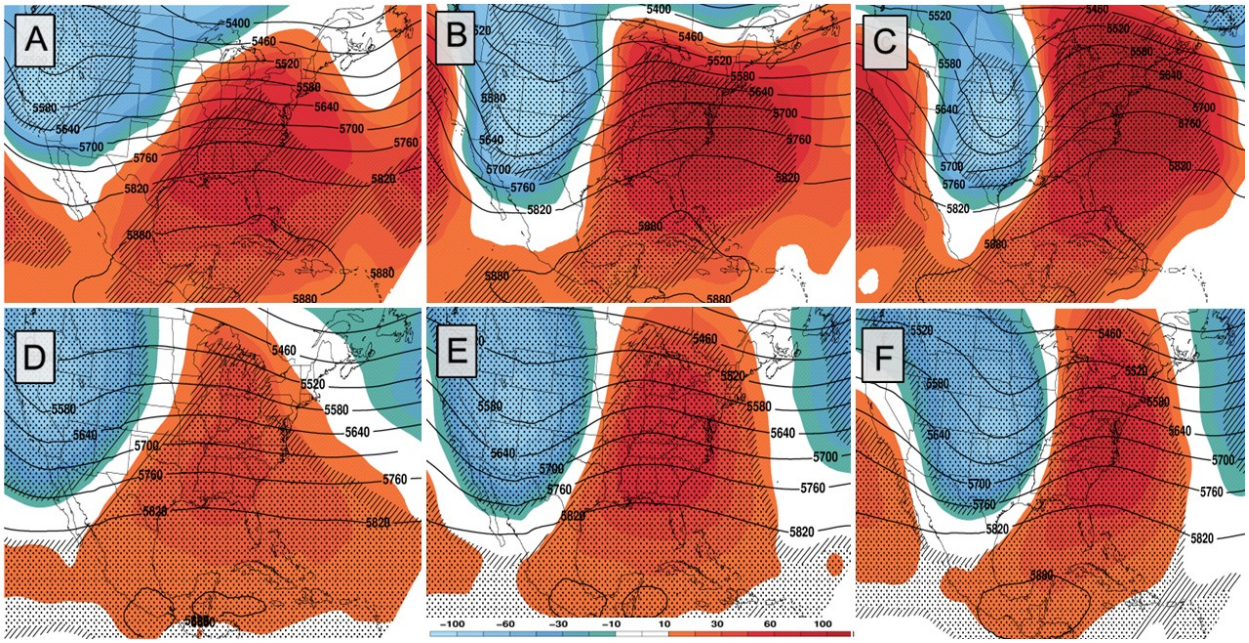

Figure 7: As in Fig. 3, but for MS events. *Click image to enlarge.*

MS and LA NULL composites had similar trough amplitudes (Figs. 2,3,6,7). In addition, the primary trough axis was located over the same geographic area in northwestern Kansas. The third similarity was the size of the PFJ and STJ streaks, an indication that both are influencing the anomalous trough by 00 h (Figs. 2 and 6f). However, the jet streak associated with LA NULL cases was stronger compared that associated with the MS NULL cases. Both NULL cases exhibited zonal flow at –48 h.

With respect to the AO, we determined (not shown) a mean +0.36 (+0.28) AO index during TOR (NULL) events, as well as a +0.14 (+0.26) standard deviation during TOR (NULL) events in the same period. However, in a three-day period, the overall change in standard deviation was only

+0.01 (+0.17). The consistency matched quite well to our MS composites (Figs. 6–9).

Additional evidence can be seen in the MS 500-hPa geopotential-height composites (Fig. 7) at the 95% and 99% confidence level, revealing a stronger STR in MS than LA at –48 h (Fig. 3). However, by 00 h, the MS STR weakened as the LA STR strengthened (see Fig. 3 and 7a–c).

The two STRs had similar anomalies (10–30 m) during MS and LA NULL cases at –48 h (Figs. 3 and 7). Both showed zonal flow across DA at –48 h (Figs. 3d and 7d). Like LA, this zonal flow is an indication of quasistationary boundaries (see Table A13). However, the ridge across DA in the MS NULL cases was slightly more amplified in comparison to the LA NULL cases. Both exhibited weaker STRs at –24 h with only MS NULL cases indicating a sign of strengthening at 00 h.

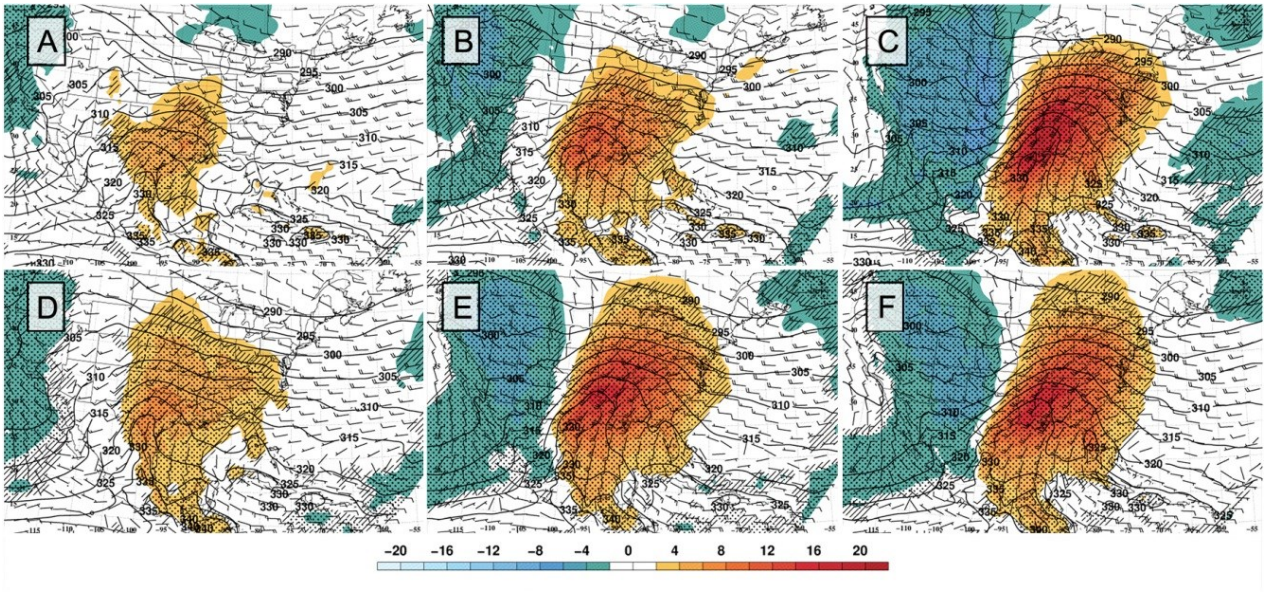

Figure 8: As in Fig. 4, but for MS events. *Click image to enlarge.*

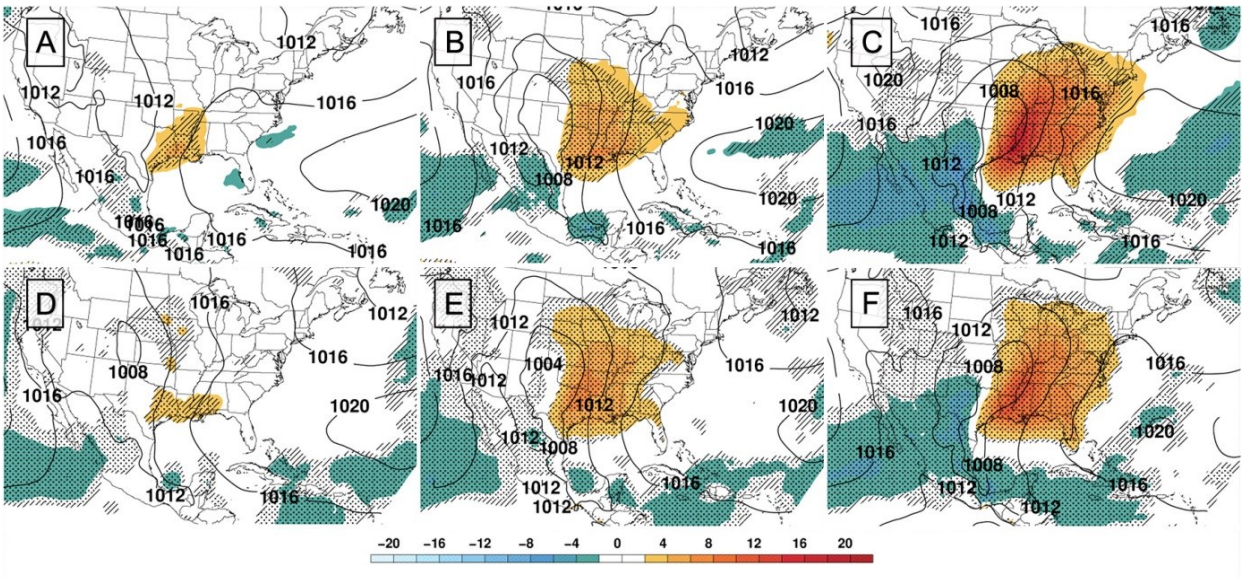

Figure 9: As in Fig. 5, but for MS events. *Click image to enlarge.*

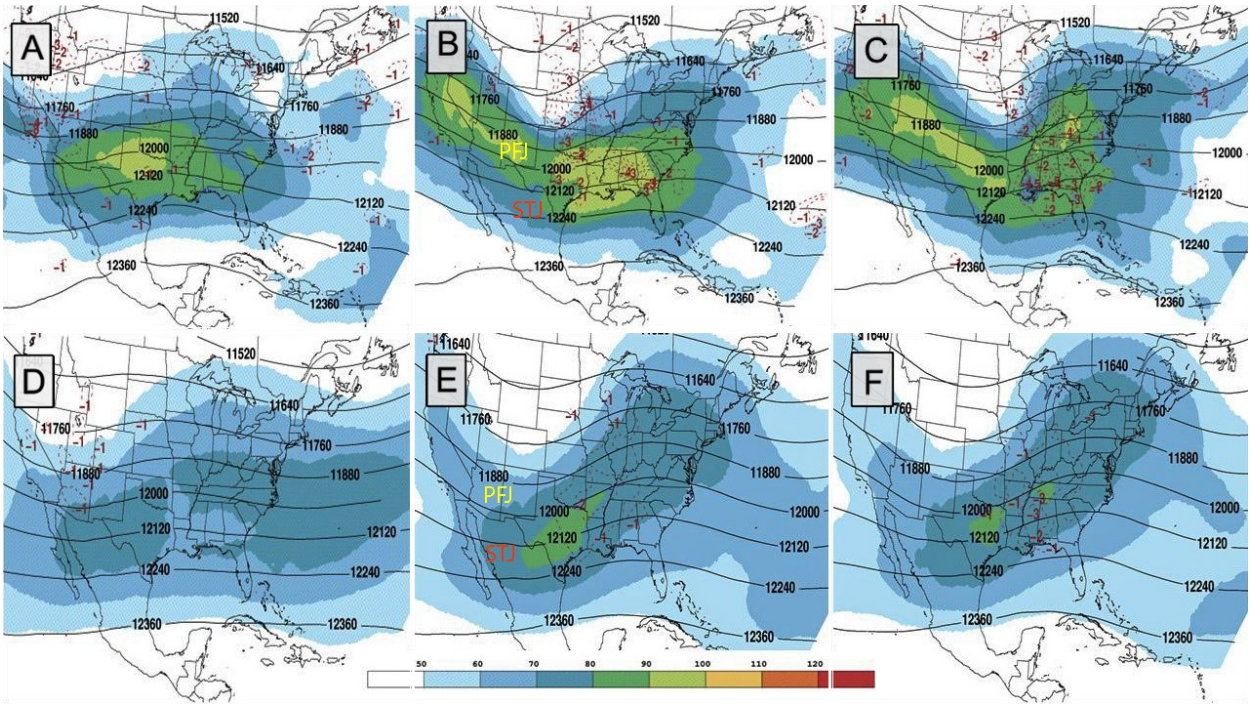

Figure 10: As in Fig. 2, but for AL events. *Click image to enlarge*.

The downstream ridge for both MS and LA cases exhibited strengthening between –48 and 00 h. However, not surprisingly, the downstream height anomalies during TOR cases were much stronger(30–45 m). The downstream ridge was displaced poleward compared to the NULL cases (Figs. 3 and 7), impacting the distance 850-hPa θ_e and W anomalies propagate For 850-hPa θ_e, LA and MS values (Figs. 4,5,8,9) were roughly the same (4 K) by –48h. However, the anomalies were far greater across MS (16 K) by 00 h. In addition, the Atlantic ridge is clearly visible on the 850-hPa θ_e plots in MS (Fig. 8). However, the Atlantic ridge is not evident in the LA composites (see Fig. 4). Therefore, the Atlantic ridge may not have much or any influence during the events across LA.

A key difference between MS and LA TOR cases is the strength of the LLJ. The LLJ during MS TOR cases averaged 40 kt (20 m s^{-1}) at –24 and 00 h, a 15-kt (≈7.5 m s^{-1}) difference from LA. However, compared to LA NULL cases, MS NULL cases were quite similar in strength and consistent with time (Figs. 4,5,8,9). MS cases had a specific timing difference in W where the NULL (TOR) cases had a maximum value at –24 h (00 h) compared to its. TOR counterparts (Fig. 9). Despite the timing, both cases had similar W values (8–12 mm).

d. Large-scale composites: AL

Another key feature at 00 h (Fig. 10c) is the jet streak weakening slightly compared to –24 h (Fig. 10b). This matched well with the 5-day average AO statistical analysis (not shown), which suggests the pattern became more amplified at –48 h (–0.148) before a gradual weakening by 00 h (–0.090). Meanwhile, substantial differences between TOR and NULL events in AL are evident in Figs. 10d–f. The mean jet streak is considerably weaker (70–80 kt and not exceeding 80–90 kt) over 48 h. However, our findings did match those found by Klepatzki and Milrad (2020), where NULL events across AL feature a less-amplified upstream trough located farther to the north than the corresponding feature during TOR events. As a result, the negative ω (-2×10^{-2} Pa s^{-1}) values are also weaker.

At –48 h, Fig. 11a shows a significantly anomalous 500-hPa ridge centered over AL with an anomalous trough approaching the Pacific Northwest. By –24 h to 00 h (Figs. 11b and c), the ridge is displaced further upstream near the Ohio Valley with a much deeper and more negatively tilted trough over the Great Plains. This suggests low-level moisture and θ_e would build over AL prior to the forward progression of this feature and

would then spread the moisture over a wider spatial area by 00 h (Figs. 12 and 13). Unlike the results of Klepatzki and Milrad (2020), the positive geopotential height anomalies in the downstream ridge decreased from 60 to 10 m between –48 h and 00 h (Figs. 11a–c) and became less significant at the 99% confidence level.

The extension of the STR over the WCR also is important. This feature weakened by 10 m between –48 and 00 h (Figs. 11a–c) and became less significant during TOR events. However, during NULL events, it maintained its intensity (Figs. 11d–f). As a result, the downstream ridge promotes strong southwesterly flow over AL prior to TOR events and southerly flow during NULL events. This ultimately affects the heat and moisture distribution over this area, which we can see in the 850-hPa θ_e and W composites (Figs. 12 and 13). W anomalies during AL and MS TOR cases were modest (4–8 mm) initially at -48 h. However, as the STR strengthened, this likely distributed increased amounts of θ_e and W across DA (see Figs. 12 and 13) between –24 and 00 h. For 850-hPa θ_e, two major differences from LA and MS cases were the 1) slightly higher amounts of θ_e at –48 h and 2) southwesterly winds by 00 h (Fig. 12) during NULL cases. However, θ_e anomalies between –48 and 00 h were similar (≥10 K), and smaller than in the MS composite (Fig. 8).

The distribution of W during NULL cases reached further poleward than during TOR cases (Fig. 13). This is perhaps due to the stronger Atlantic ridge (Fig. 13), which has more of an influence in AL cases than LA cases. We assume the stronger Atlantic ridge focuses W over AL, which is evident at –24 h (Fig. 13b). The poleward extension of W at 00 h is likely due to the east-northeast movement of the anomalous trough (Figs. 10 and 11).

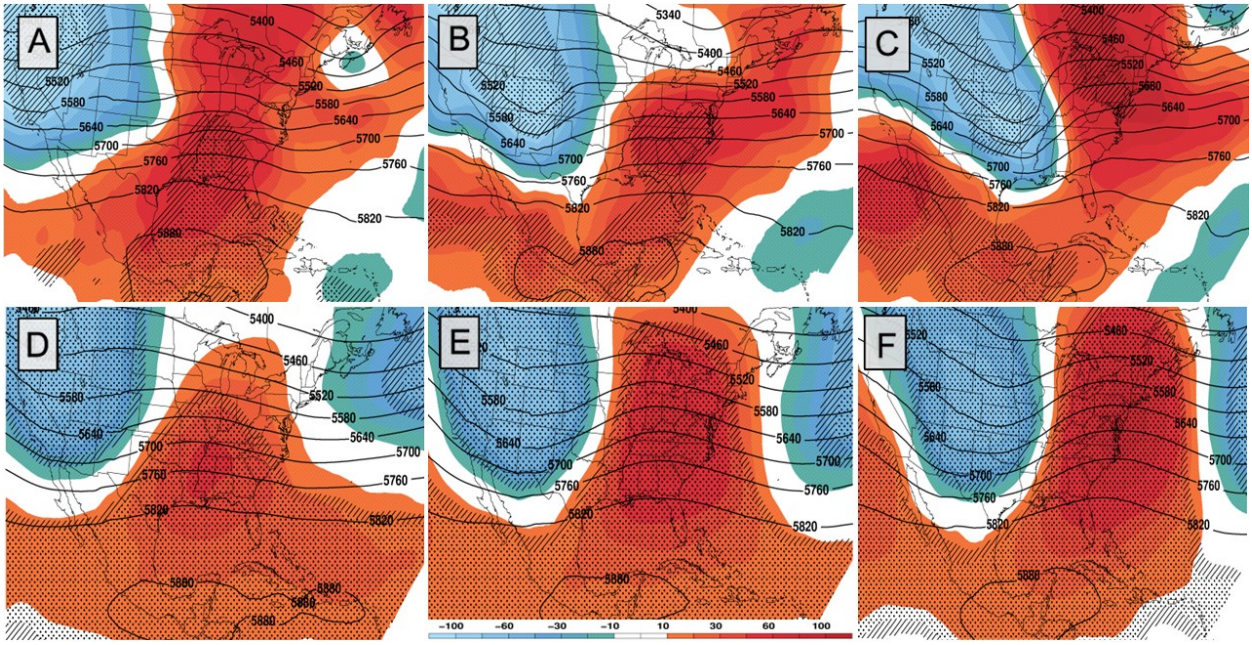

Figure 11: As in Fig. 3, but for AL events. *Click image to enlarge*

e. Large-scale composites: GA

Previous studies (Armstrong 1953; Stakely 1957) identified the relative time of occurrences and typical height maps seen during GA TOR events. Armstrong (1953) was perhaps the first to reveal these conditions, including the mean location of tornadoes that occurred over GA from 1884–1952. Armstrong's findings and the QGIS analysis described earlier (see section 2) were similar. However, compared to our study Armstrong favored a poleward position. Stakely (1957) would later update Armstrong's findings by providing a mean frontal analysis during TOR events. Stakely (1957) found a surface thermal ridge in place specifically when a stationary front or a QLCS boundary were noted.

Comparing GA 200-hPa composites to the rest of DA, there are multiple similarities. First, like LA,

GA had the most west–east oriented jet streak (Fig. 14a) at –48 h. Second, both were considerably weaker in magnitude (70–80 kt) which corresponded to the smaller ω (-1×10^{-2} Pa s^{-1}) values (Fig. 14a). Third, the broad nature of this feature matches the PFJ and STJ maintaining the lifecycle of the anomalous trough mentioned earlier. However, unlike LA and MS (Figs. 2c and 6c), the jet-streak magnitudes (Fig. 14c) were similar to AL events (90–100 kt) at 00 h (Figs. 10c and 14c). Also, the anomalous trough amplified over 48 h, yet remained much weaker in comparison to the rest of DA. As a result, this led to the consistent west–east oriented jet streak (Fig. 14). Despite this, ω (-5×10^{-2} Pa s^{-1}) values were smaller than those in AL (-6×10^{-2} Pa s^{-1}) yet, larger than those found (-4×10^{-2} Pa s^{-1}) by Klepatzki and Milrad (2020) over FL during a TOR event. However, these values did match those found by Klepatzki and Milrad (2020) for FL NULL events. Thirdly, the anomalous trough in NULL events was more amplified than in TOR events and is like those observed in LA and MS at 00 h (Figs. 2 and 6, respectively).

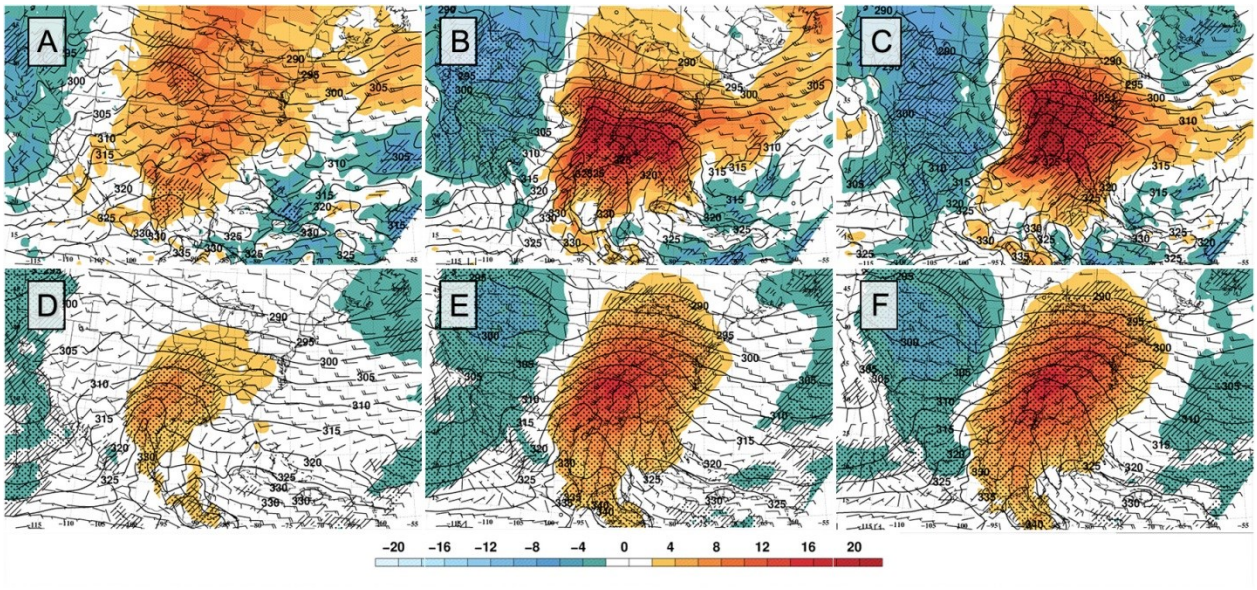

Figure 12: As in Fig. 4, but for AL events. *Click image to enlarge*.

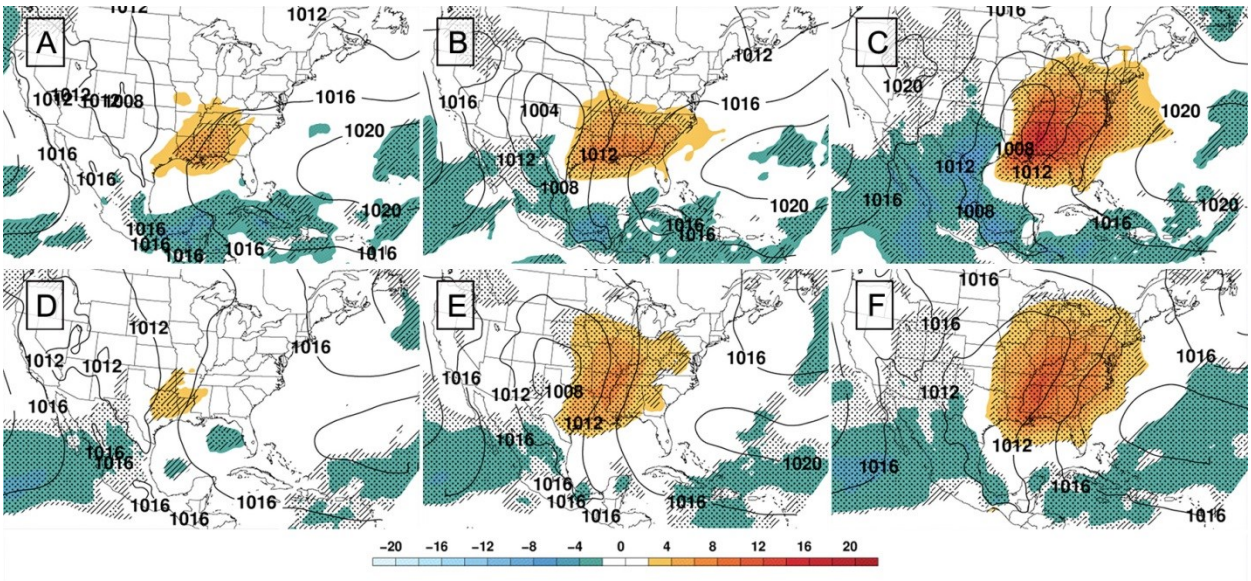

Figure 13: As in Fig. 5, but for AL events. *Click on image to enlarge.*

Regarding our AO statistical analysis, NULL events in GA were more similar (+0.53) to those found in AL (+0.49) than MS and LA. The opposite can be said for TOR events, which had a more neutral (–0.02) pattern than MS and AL, with LA as a close second. This reflects the consistent zonal jet stream mentioned earlier. Amplification of the anomalous trough (see Fig. 14f) in NULL events is supported by the statistical analysis that showed an AO change of –0.06 in 24 h. The lack of amplification in TOR events was noted as the AO changed by +0.02 during the same period. Therefore, showing changes in AO values can correlate to the shape of the overall synoptic structure.

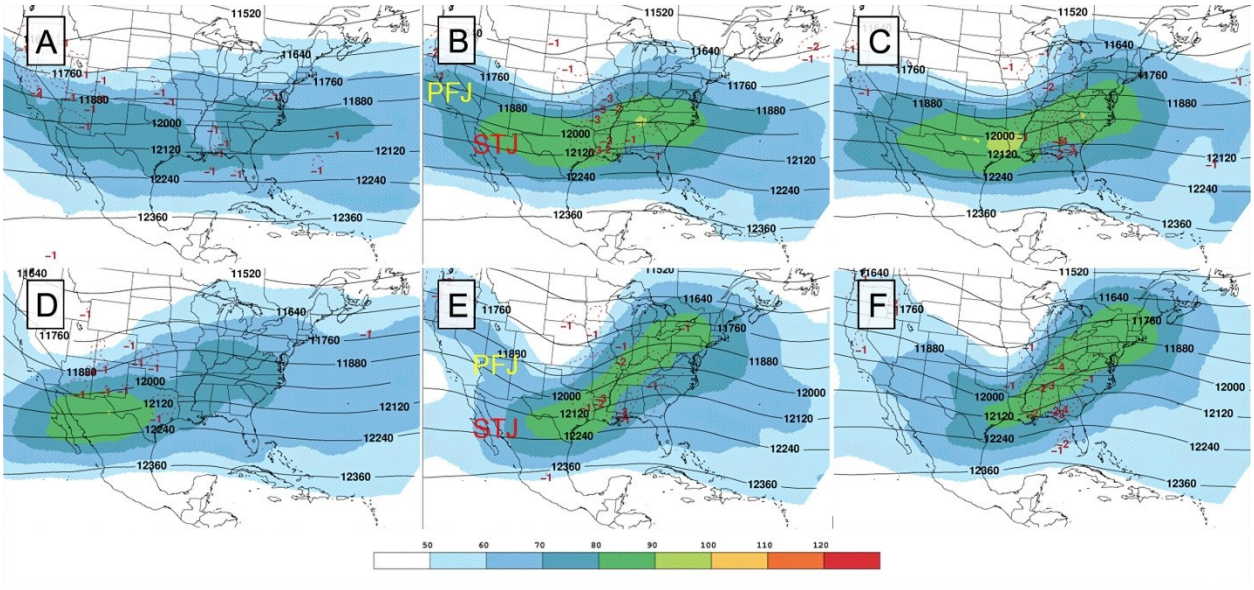

Figure 14: As in Fig. 2, but for GA events. *Click image to enlarge.*

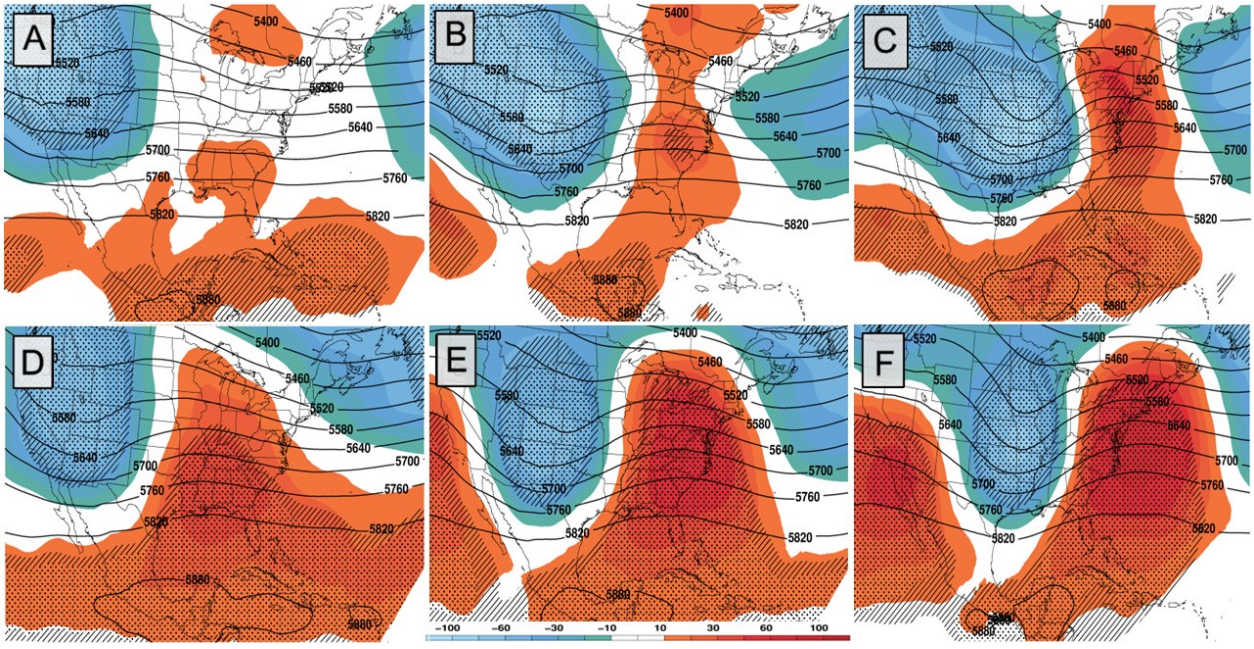

Figure 15: As in Fig. 3, but for GA events. *Click on image to enlarge.*

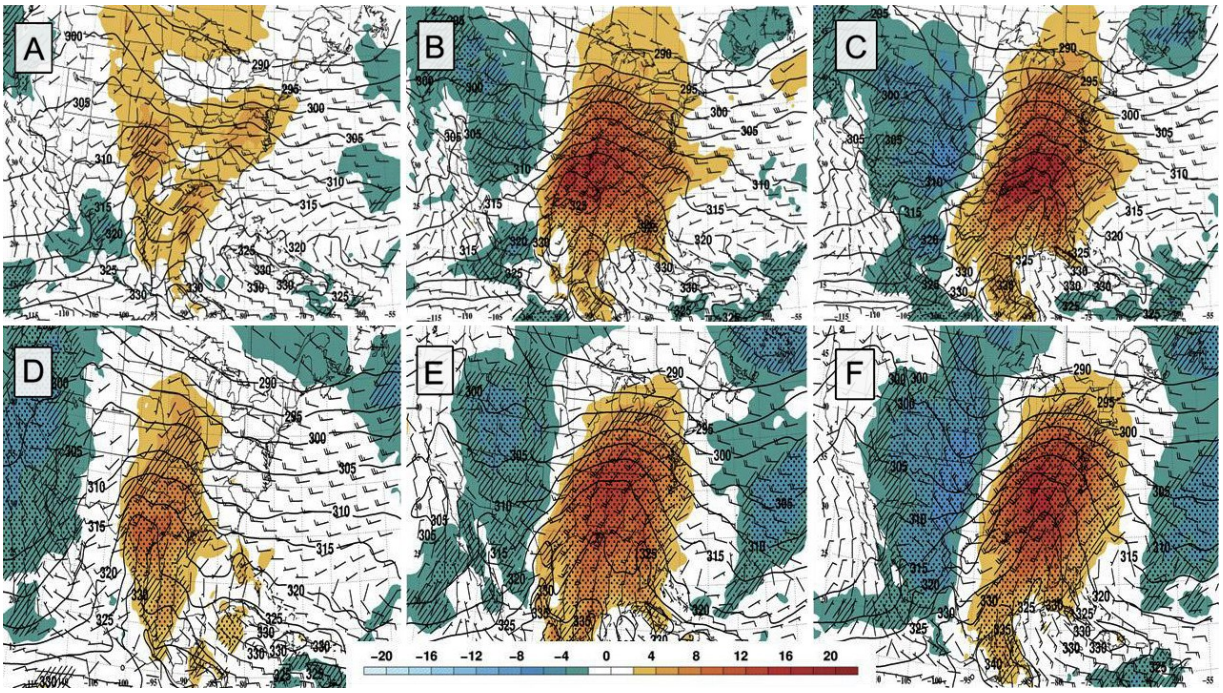

Figure 16: As in Fig. 4, but for GA events. *Click on image to enlarge.*

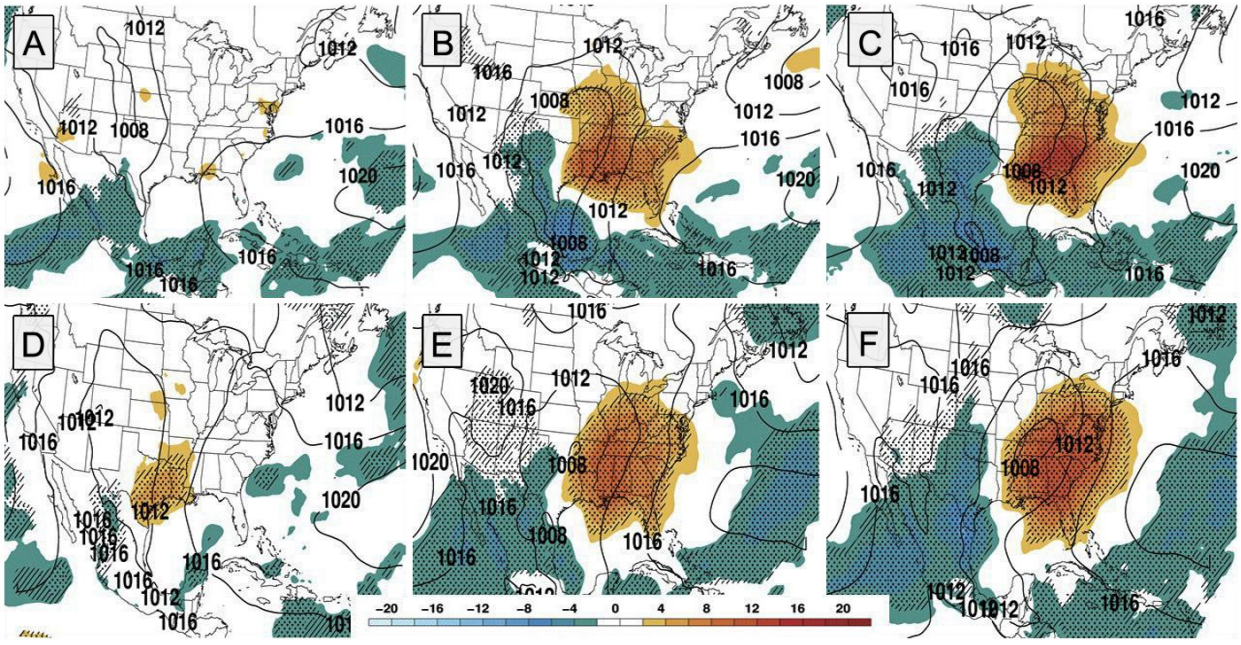

Figure 17: As in Fig. 5, but for GA events. *Click on image to enlarge.*

Comparing GA to LA, the 500- and 850-hPa composites showed strong DPVA across DA (Figs. 3, 4, 15 and 16). For TOR events, there was an initial anomaly of 10 m at –48 h (Fig. 15a). However, geopotential heights over GA decreased by 10 m and became less significant at the 99% confidence level at 00 h (Fig. 15c). This is not a surprise, since TOR events in AL (Fig. 11) exhibited similar behavior as the upstream trough became negatively tilted.

The STR during TOR events of GA is substantially different than in our other states. For example, in the WCR and eastern Cuba, a double positive height anomaly existed in the STR, and strengthened during this same period (Fig. 15c) by 10 m. This would keep winds out of the west - southwest, thus advecting large amounts of θ_e and W (Figs. 16 and 17) from the Yucatan over a modest spatial area. It would also act as a limiter, thus preventing events from taking place in Florida as θ_e and W from the central Caribbean Sea would contain lower amounts in comparison (Figs. 16 and 17) and be advected further to the north. Like LA, θ_e advection and W support the findings of Molina and Allen (2019).

This one difference also makes GA unique compared to the findings of Klepatzki and Milrad (2020). For example, Klepatzki and Milrad (2020) noted a single STR height anomaly existed near Haiti when a TOR event was occurring over Florida. The existence and strengthening of the 500-hPa STR plays a vital role in TOR events across DA.

NULL events describe a different story. For example, the 500-hPa geopotential height anomalies initially are stronger (≥30 m) at –48 h (Fig. 15d) before becoming less significant (≤ 10 m) at the 99% confidence level at 00 h (see Fig. 15f). Unlike TOR events, NULL events only exhibited one STR anomaly throughout the Caribbean Sea during the 48-h period (Figs. 15d—f), specifically the WCR. This was the one common signature found by Klepatzki and Milrad (2020) during NULL events.

Accordingly, W composites showed minimal anomalies initially at –48 h (Figs. 17a,d) for both TOR and NULL events. However, during TOR events, W increases (8–12 mm) and becomes more concentrated by 00 h (Fig. 17c). W in NULL events also increases while remaining generally less concentrated (4–8 mm), and spread over a larger spatial area (Fig. 17f). These concentration differences correlate well to the overall storm reports (Fig. 1) and event climatology described earlier.

4. Conclusions and future studies

A multiscale environmental analysis of 33 AL tornado and 65 null events; 46 MS tornado and 92 null events; 24 LA tornado and 98 null events; and 21 GA tornado and 32 null events across DA was conducted using the NARR. Our work to examine the large-scale conditions associated with tornado events over relatively narrow geographic regions corresponds with studies such as Netherton and Lanicci (2024), who focused on a sub-region of AL.

We also conducted a statistical analysis of the tornado reports using QGIS, elucidating the geographical climatology of enhanced or higher risk events. Specifically, these events occur more frequently over the central and northern regions of each state. These areas on average include higher concentrations of mobile homes and tend to be well developed. The higher developed areas also provide increased threat to human life and personal property, corresponding to Anderson-Frey et al. (2016, 2019) and the CDC SVI.

Our synoptic-scale composite analysis (sections 3b–e) also showed that the lifecycle of the anomalous trough(s) is supported by more than one jet stream (STJ and PFJ) over a 48-h period. The associated jet streaks varied in magnitude from state to state, with some states (i.e., AL; MS; GA) sharing similarities to others (FL) despite being more tornadic. Similarities to the findings of Klepatzki and Milrad (2020) for FL include TOR (NULL) events being associated with stronger (weaker) jet streaks. However, TOR and NULL events in other states (e.g., LA) differed greatly in trough orientation and amplification, including jet-streak magnitude.

The support by multiple jet streaks also revealed a longer life cycle of the anomalous trough(s). Trough amplitude would dictate its equatorward or poleward placement. In terms of the wind-shear vector, an increasing poleward position of the surface cyclone would favor a QLCS event.

A coupled jet-streak divergence region is another common feature found across the Southeast. Composites in this paper and those noted by Klepatzki and Milrad (2020) revealed such areas can affect overall ascent forcing. However, the composites also illustrated such areas of maximum ascent can vary. Our composites also revealed that some states (LA; GA) have more zonal jet streaks in nature compared to others (AL; MS). Previous documentation (Porter et al. 1955) showed similar results for squall-line formations across the Central U.S., particularly when conditions were less amplified, with a 500-hPa ridge nearby and in areas of 50 kt (≈25 m s^{-1}) near jet streaks.

Though this is out of our area of interest, these techniques proved to be beneficial during their study of dynamic and thermodynamic comparisons.

Compared to Klepatzki and Milrad (2020), our synoptic-scale composite analysis also showed distinct differences in 500-hPa geopotential height anomalies. The differences of these features were dependent on timing, strength, location and surprisingly, the number of height maxima. While on average TOR or NULL events across the Southeast had one height maximum over the WCR or Haiti, GA remains as the only state with two height maxima across both areas. As a result, the western anomaly would limit W and θ_e anomalies across other states in DA by providing northerly winds, while the eastern anomaly would enhance W and θ_e anomalies with southerly winds across areas of the east coast. The limit or enhancement of θ_e anomalies combined with surrounding cooler than average SSTs would allow potential convergence zones to develop, and enhance mesoscale forcing and storm-relative helicity during high θ_e advection. This was also echoed by many others (e.g., Wasula et al. 2007; Lee et al. 2016; Molina et. al. 2016, 2018). Given the importance of the 500-hPa height anomalies over the Caribbean Sea, one avenue to explore in the future is the AMO. This analysis may reveal the variability of the STR, which in turn may offer useful relationships to DA severe weather events.

Investigating the 500-hPa geopotential height anomalies revealed orientations of these features varied from state to state. This could offer an important clue for future severe-weather forecasts. These height anomaly changes showed winds remained out of the west-southwest over the Southeast, which matched the findings of previous studies (Gaffin and Parker 2006; Klepatzki and Milrad 2020). Another key feature is the consistency of the LLJ. As a result, θe and W also increased over our 48-h composite period, matching the results of Molina and Allen (2018). The consistent increase in θe and W was argued by Klepatzki and Milrad (2020) as helpful for severe events.

Another variable that we investigated is the daily change of the AO. While we are not making broad, statistically significant conclusions, we have shown some correlation between the different phases of AO and the orientation of jet streaks and synoptic features. Therefore, future studies will be done on other tornado-prone regions by conducting a similar analysis. For example, we briefly investigated another state, Arkansas. Utilizing AO daily data (not shown), we found Arkansas had an average TOR (NULL) event of –0.59 (+0.52) from 2002–2004. Though this was not like our LA results, it was similar to our GA results. Surprisingly, despite the small sample size, Arkansas shared a similar TOR/NULL case ratio to those of LA. This suggests teleconnection patterns conducive for specific severe weather patterns vary from state to state or subregion to subregion. To that end, another teleconnection worth exploring with respect to Southeast/DA tornado events is the Trans Nino Index (TNI), as detailed by Lee et al. (2013).

Perhaps the most crucial future study that can be done is the analysis of SPC enhanced- or higher-risk events during specific jet-streak magnitudes. One such event (e.g., 18 May 2017) had a strong jet streak of 100 kt ($\approx$50 m s^{-1}) which was associated with more tornadoes in the adjacent state than within the higher-risk areas (i.e., Kansas and Oklahoma). However, future studies could also include the application of climate zones for each respective state based on specific risk events, resulting in greater event detail and improved forecasting capabilities. For example, if we were to focus on a narrower area, it could lead to ascertaining finer details of severe weather environments once grid resolution(s) improve. Finally, the composite analysis completed in this study could be reproduced using objective synoptic typing or machine-learning methods, to serve as a point of comparison.

ACKNOWLEDGMENTS

The authors would like to thank NOAA SPC for the available archived storm reports and the NOAA National Center for Environmental Information (NCEI) for making the NARR data available. Teleconnection data were downloaded from the NOAA CPC archives. Storm reports were mapped using ESRI's QGIS. The composite analysis was performed using Unidata's General Meteorological Package (GEMPAK) Version 7.4.3. This research was partially supported by the Embry-Riddle Aeronautical University Applied Aviation Sciences Department. Finally, the authors express their deepest gratitude toward the two reviewers and the editor for their time and patience.

APPENDIX A

Table A1: Dates and time periods (UTC) of the 24 LA TOR events from the first to last TOR report. Shaded boxes represent nighttime occurrences.

Date	Time (UTC)	Number of Tornadoes
20030318	2320–0114	7
20030424	2100–2115	4
20030506	0739–1050	4
20050406	1335–1845	9
20070224	1642–0155	7
20081209	1552–1832	9
20110308	0047–1145	12
20110426	0034–0636	18
20121225	1843–0020	9
20150427	1415–1523	6
20151227	0210–0920	5
20160223	1656–0114	21
20170102	1606–2044	9
20170121	2312–0304	9
20170207	1625–1755	8
20170324	0305–0454	5
20170402	1404–0917	26
20170429	1924–0950	5
20180406	2304–1018	9
20180413	1212–1137	25
20180414	1313–1413	5
20190413	2104–0009	7
20190508	2033–2352	15
20191216	1610–2146	12

Table A2: Dates and time periods (UTC) of the 98 LA NULL events from the first to last hail/wind report. Maximum SPC 0600 UTC Day 1 tornado probability (%) over AL is shown in the right-hand column. Shaded boxes represent nighttime occurrences.

Date	Time (UTC)	Maximum Tornado Probability (%)
20020330	0135–1145	15
20021218	2230–0255	15
20021219	1820–0110	15
20021223	1945–0725	30
20021230	0155–0940	15
20030221	0532–0550	15
20030406	1220–0525	25
20030503	2244–2323	5
20030504	2320–0655	15
20030505	1038	15
20030510	2040–0838	5
20030516	0055–1140	15
20040304	0130–0230	5
20040530	2000–0545	15
20041206	0345–1134	15
20050321	0250–1055	15
20050326	2100–2334	15
20050330	1409–1015	15
20050331	2315–0815	5
20050405	0425–1022	5
20050411	1245–2355	25
20050422	1602–0008	5
20050429	0233–1157	5
20060113	1355–1505	5
20060308	1740–1145	10
20060309	1430–1845	15
20060311	2102–0707	15
20060320	1710	15
20060407	2010–0650	15
20070301	1345	15
20070413	2200–0900	15
20070414	1200–1655	15
20070424	1140	15
20080110	1600–1915	15
20080205	0051–0956	15
20080216	1205–1110	10
20080303	1720–0447	15
20080318	0523–1024	15
20080403	1624–1030	5
20080410	2030	10
20080502	1946–1125	10
20080507	0150–0400	15
20080510	0410–0453	15
20090210	0710–0910	15
20090218	2305–0231	10
20090327	2000–0435	10

Date	Time (UTC)	Maximum Tornado Probability (%)
20090402	1342–1842	15
20090503	1238–1155	5
20091224	1300–1654	15
20100423	1736–1157	15
20100424	1223–1623	30
20100430	2043–0815	10
20100501	1910–0325	10
20110224	2230–0150	15
20110404	1838–0145	5
20110415	1314–2245	10
20110425	0058–1055	15
20120122	0019–0410	15
20120302	1940–0250	5
20130129	1453–0740	15
20130521	0015–0330	10
20131221	1732–2333	15
20140403	0615–1105	10
20140427	0809–0822	10
20140428	1805–2205	15
20140429	2105–2205	15
20141223	1506–1959	10
20150403	2244	5
20150409	0045	5
20150419	2325–0319	5
20150424	1745–0535	10
20150509	2100–0735	5
20150510	1555–0720	5
20150525	2105–0937	10
20151223	1316–2043	15
20160108	0135–0605	5
20160121	1252–0005	10
20160313	0042–0345	5
20160317	1900–0412	5
20160330	0115–1114	10
20160331	1950–2240	5
20160411	2012–2130	5
20160429	1725–0612	10
20160509	0000–0610	5
20170120	0445–0513	5
20170329	2218–0320	10
20170426	2100–0028	15
20170430	1214–1723	5
20170503	1223–0742	5*
20180224	1911–0019	10
20180403	2040–0524	5
20190223	2213	10
20190313	2330–1025	5
20190324	0809–0813	5
20190406	1633–0935	5
20190407	1314–0122	5
20190418	1407–0036	10
20190518	0702–1145	10

Table A3: Same as A1, but for 46 TOR events across MS.

Date	Time (UTC)	Number of Tornadoes
20030406	1650–0037	9
20030424	2120–0400	8
20041206	0700–0955	15
20050322	1306–2324	5
20050326	2230–0040	6
20050406	1224–0210	34
20050429	0215–0915	7
20060320	1830–2210	5
20060407	2125–0255	14
20060510	1820–2344	5
20070224	0005–0440	5
20070414	1510–1641	4
20080110	1708–2058	17
20080205	2245–0755	18
20080303	2150–0615	15
20080502	1233–0550	18
20081209	2123–0713	24
20090402	1742–0028	6
20090503	1200–1135	7
20100424	1340–0032	38
20100501	1834–0829	9
20110404	1845–0145	8
20110415	1520–0055	45
20110426	1212–0903	43
20110427	1415–0000	54
20110525	0020–0140	4

Date	Time (UTC)	Number of Tornadoes
20120122	0434–0853	4
20121225	2032–2235	20
20130418	2204–2230	7
20131221	2319–2357	4
20140428	1857–0315	94
20141223	2017–2227	17
20150103	2005–2253	13
20151223	2054–0140	15
20160121	2214–0051	6
20160202	2048–0039	15
20160223	2145–2345	18
20161217	0315–0453	5
20170102	1902–2128	14
20170120	0935–1005	6
20170430	1224–1643	38
20180406	0103–0433	10
20180414	1244–2339	11
20190223	2240–2317	6
20190309	1931–2317	4
20190413	2157–0755	26
20190418	1812–2242	57
20191216	1724–0107	40

Table A4: Same as A2, but for 92 NULL events across MS.

Date	Time (UTC)	Maximum Tornado Probability (%)
20020329	0430–0720	15
20020330	0115–0920	15
20020427	0745–1137	5
20021218	0750	15
20021219	1530–2020	15
20021223	0245–1000	30
20021224	1240–1300	15
20030221	0200–0600	15
20030318	0119–0545	15
20030404	0400–1105	15
20030425	2008–0458	15
20030503	1200–2336	15
20030504	0900–1153	15
20030505	1255–0725	15
20030506	0135–1145	5
20030510	0745–0835	15
20030516	0315–1156	15
20040304	0130–0230	5
20040530	0305–0755	15
20050321	0250–1055	15
20050327	2127	15
20050330	1409–1015	15
20050331	2315–1050	5
20050411	1245–2355	25
20050421	0820–1130	5
20050422	1225–0210	5
20060113	1300–1315	5
20060309	1740–2240	15
20060312	0416–0840	5
20060402	2259–0915	15
20070301	1700–2216	30
20070403	2317–0925	5
20070413	2315–1150	10
20080318	0548–1024	10
20080410	0145–0735	10
20080510	0045–0531	15
20090218	2305–0231	10
20090327	2335–0900	10
20090410	1638–1823	5
20090412	1823–0404	15
20091224	1841–2150	15
20100423	2020–1145	15
20100430	0127–0900	10
20110224	0127–0518	15
20110227	0520–0605	5
20110228	1746–0136	15
20110308	2019–1145	15
20110326	1828–0406	15
20110411	2220–0303	10
20110419	0341–0915	5
20110420	1204–0504	5
20110425	0315–1140	15
20120229	2150–2245	15
20120302	1938–0547	15
20130129	0127–1130	15

Date	Time (UTC)	Maximum Tornado Probability (%)
20130521	2350–0525	5
20140220	2205–0552	5
20140403	0705–0946	10
20140427	1203–2237	15
20140429	2105–2159	15
20150403	2220–0150	5
20150409	0615–1050	5
20150419	0215–0525	5
20150424	0446–0850	5
20150427	1205–2325	5
20160313	0313–0456	10
20160317	1344–0907	5
20160330	2150–0044	10
20160331	1253–0638	10
20170121	0040–0529	10
20170207	1750–0015	5
20170301	1844–2107	5
20170327	1640–0122	5
20170329	1758–1110	10
20170330	1530–1647	10
20170402	1624–1045	15
20170403	1210	5
20170404	0550–1140	10
20170405	1239–0307	5
20170426	0045–0608	10
20170503	1223–0742	5
20170527	0500–0645	5
20180224	0108–0415	10
20180319	1615–2220	10
20180403	2336–0357	5
20180413	1630–1155	10
20190303	1655–1728	5
20190313	0125–0306	5
20190314	1849–2107	5
20190406	2040–0245	5
20190407	1817–0135	5
20190518	0913–0929	5

Table A5: Same as A1, but for 33 TOR events across AL.

Date	Time (UTC)	Number of Tornadoes
20021224	1240–1300	5
20060113	1601–1855	4
20060407	2241–0703	28
20060510	1944–2315	5
20070301	1830–2355	30
20070414	1838–0005	6
20080110	1908–2221	8
20080510	0400–0747	8
20090402	2019–0109	8
20090410	1856–0227	16
20090503	1823–2300	12
20100424	1544–0515	14
20110228	1818–2337	5
20110415	1614–0610	84
20110427	1629–0248	86
20120122	0836–1135	21
20120302	1510–0440	30
20121225	2115–0429	26
20140220	0251–0756	6
20140428	2056–0856	46
20150103	2206–0932	7
20160202	2231–0507	13
20160223	2220–1004	17
20160331	2332–0523	22
20170102	2224–0147	6
20170121	1355–0636	14
20170122	1900–2000	4
20170405	1449–0139	4
20180319	2205–0209	23
20190223	2344–0754	6
20190303	1855–2253	22
20190314	2110–0300	24
20191216	2252–0411	12

Table A6: Same as A2, but for 65 NULL events across AL.

Date	Time (UTC)	Maximum Tornado Probability (%)
20021219	1530–2020	15
20030221	0625–1130	15
20030222	1215–1130	25
20030406	2040–1000	25
20030425	1730–0400	5
20030503	1240–2045	5
20030504	1015–1110	15

Date	Time (UTC)	Maximum Tornado Probability (%)
20030505	1644–1157	25
20040530	0453–0800	15
20050322	1435–0630	15
20050326	1735–0835	15
20050327	1727–2114	15
20050330	1526–1145	15
20050331	1220–1104	5
20050406	1912–0457	15
20050422	1445–0323	15
20050429	0717–1145	15
20060102	1230–0230	15
20060309	2117–0020	15
20060320	0000–0230	15
20060402	0719–1146	15
20070224	0308–0520	15
20070403	1715–0824	5
20080205	0804–1145	15
20080303	0649–0944	15
20080315	1225–2037	15
20080410	0023–0636	10
20090218	1300–0450	10
20090327	1200–1130	5
20091224	2240–2345	15
20100501	2007–0116	15
20110224	0405–0735	15
20110326	1828–0330	15
20110404	1857–0515	5
20110411	2220–0303	10
20110426	2220–1155	5
20110525	0430–0544	15
20120229	2221–2238	15
20130129	0830–1156	15
20130418	0614–0720	10
20131221	0255–0412	10
20140429	2335–0850	15
20141223	1410–0256	10
20150403	2336–0232	5
20151223	1230–0610	15
20160121	0500–0725	10
20160317	1913–0202	5
20161217	1739–0815	5
20170120	1114–1153	5
20170207	1942–2230	5
20170301	1757–0016	5
20170321	2304–0033	5
20170327	1927–0257	5
20170330	1640–1909	5
20170402	0848–1145	5
20170403	1200–1548	5
20170404	0550–1140	5
20170430	1629–2035	5
20170527	0310–0834	5
20180224	0600–0623	5
20180403	1642–0540	5
20180414	1338–0211	10
20190309	2207–0115	10
20190413	0456–1157	10
20190418	2136–1030	10

Table A7: Same as A1, but for 21 TOR events across GA.

Date	Time (UTC)	Number of Tornadoes
20021224	1320–0145	15
20030319	0215–1040	7
20030425	1754–2235	6
20050322	1850–2130	8
20060102	1723–0212	11
20060113	1938–0130	4
20060407	0720–0815	9
20070301	1635–0758	27
20080315	1624–0143	20
20080510	0805–1140	29
20080511	1210–1959	6
20090218	2245–0715	20
20090410	2100–0540	22
20110427	1240–0739	46
20120302	0109–0214	7
20160223	0507–0749	6
20170121	1541–0925	41
20170122	1200–2329	12
20170403	1458–1917	47
20170405	1609–1942	12
20190303	2015–0057	40

Table A8: Same as A2, but for 32 NULL events across GA.

Date	Time (UTC)	Maximum Tornado Probability (%)
20021231	1230	5
20030221	0625–1118	5
20030222	1215–1836	5
20030320	1442–0120	15
20030505	1829–0255	5

Date	Time (UTC)	Maximum Tornado Probability (%)
20050326	2251–0930	15
20050327	1640–0200	15
20050401	1255–2030	5*
20050422	1535–2350	15
20060403	1215	10
20070414	2225–1115	15
20080304	1715–0105	15
20090402	1245–0420	15
20090503	2100–0024	5
20100424	1606–1005	30
20110228	1930–2325	10
20110326	1645–1026	15
20110404	2200–1036	5
20110415	2034–1022	15
20120229	2147–0800	15
20140428	2300–1000	15
20150403	0210–0220	5
20151223	1046–1055	5
20160331	2218–1149	10
20170301	2047–0125	10
20170321	2000–0328	5
20170524	1344–0437	5
20170527	1625–1020	5
20180319	1900–0731	10
20180320	1810–1900	10
20180415	1240–1900	10
20190419	1200–0335	10

Table A9: The date of each LA tornado event, two-month mean MEI and CPC ONI, and daily AO index. Gray shading indicates nighttime outbreaks, while yellow and blue shading indicate the ONI/AO threshold was met for positive and negative ENSO/AO events, respectively.

Date	MEI	CPC ONI	Daily AO Index
20030318	0.06	0.4	–0.19
20030424	0	–0.3	–2.29
20030506	–0.5	–0.3	1.4
20050406	0.1	0.4	–0.24
20070224	0.5	0.3	–1.23
20081209	–1.1	–0.7	0.85
20110308	–1.8	–0.8	1.74
20110426	–1.9	–0.6	1.35
20121225	0	–0.2	–1.25
20150427	0.5	0.8	–0.59
20151227	1.9	2.6	1.81
20160223	1.8	2.2	–0.76
20170102	–0.2	–0.3	0.05
20170121	–0.2	–0.3	0.93
20170207	–0.2	–0.1	–1.00
20170324	–0.5	0.1	1.82
20170402	–0.4	0.3	1.98
20170429	–0.4	0.3	–0.3
20180406	–1.3	–0.4	–1.7
20180413	–1.3	–0.4	0.13
20180414	–1.3	–0.4	0.98
20190413	0.3	0.7	0.05
20190508	0.2	0.6	–1.78
20191216	0.4	0.5	–1.12

Table A10: Same as A9, but for MS.

Date	MEI	CPC ONI	Daily AO Index
20030406	0	0	0.39
20030424	0	0	–2.29
20041206	0.5	0.7	0.88
20050326	0.8	0.4	–1.00
20050406	0.1	0.4	–0.24
20050429	0.1	0.4	–2.39
20060320	–0.6	–0.5	–3.5
20060407	–0.8	–0.3	–2.37
20060510	–0.3	–0.3	1.25
20070224	0.5	0.3	–1.23
20070414	–0.5	–0.2	0.87
20080110	–1.1	–1.6	–0.6
20080205	–1.2	–1.4	1.00
20080303	–1.6	–1.2	–0.02
20080502	–1	–0.8	–2.92
20081209	–1.1	–0.7	0.85
20090402	–0.7	–0.2	0.89
20090503	–0.6	0.1	2.08
20100424	0.4	0.4	–1.33
20100501	–0.5	–0.1	0.32
20110404	–1.9	–0.6	3.88
20110415	–1.9	–0.6	2.49
20110426	–1.9	–0.6	1.35
20110427	–1.9	–0.6	0.7
20110525	–1.3	–0.5	0.31
20120122	–1.1	–0.8	–2.01
20121225	0	–0.2	–1.27
20130418	–0.4	–0.2	2.32
20131221	–0.3	–0.3	3.03
20140428	–0.2	0.1	–1.11
20141223	0.3	0.7	0.56
20150103	0.2	0.6	1.83

Date	MEI	CPC ONI	Daily AO Index
20151223	1.9	2.6	3.93
20160121	1.9	2.5	–1.06
20160202	1.8	2.2	0.89
20160223	1.8	2.2	–0.76
20161217	–0.2	–0.6	1.43
20170102	–0.2	–0.3	0.05
20170120	–0.2	–0.3	1.72
20170430	–0.4	0.3	–0.85
20180406	–1.3	–0.4	–1.7
20180414	–1.3	–0.4	0.98
20190223	0.5	0.8	1.69
20190309	0.7	0.8	2.49
20190413	0.3	0.7	0.05
20190418	0.3	0.7	0.16
20191216	0.4	0.5	–1.12

Table A11: Same as A9, but for AL.

Date	MEI	CPC ONI	Daily AO Index
20021224	0.8	–0.3	–0.73
20060113	–0.7	–0.8	1.47
20060407	–0.8	–0.3	–2.37
20060510	–0.3	0	–1.02
20070301	–0.1	0	0.11
20070414	–0.5	–0.2	0.87
20080110	–1.1	–1.6	–0.6
20080510	–1	–0.8	–1.19
20090402	–0.7	–0.2	0.89
20090410	–0.7	–0.2	0.66
20090503	–0.6	0.1	2.08
20100424	0.4	0.4	–1.33
20110228	–1.6	–1.1	0.9
20110415	–1.9	–0.6	2.49
20110427	–1.9	–0.6	0.7
20120122	–1.1	–0.8	–2.01
20120302	–0.6	–0.5	1.14
20121225	0	–0.2	–1.27
20140220	–0.4	–0.4	0.74
20140428	–0.2	0.1	1.11
20150103	0.2	0.6	1.83
20160202	1.8	2.2	0.89
20160223	1.8	2.2	–0.76
20160331	1.3	1.7	1.18
20170102	–0.2	–0.3	0.05
20170121	–0.2	–0.3	0.93
20170122	–0.2	–0.3	0.32
20170405	–0.4	0.3	0.38
20180319	–0.9	–0.6	–0.25
20190223	0.5	0.8	1.69
20190303	0.7	0.8	2.38
20190314	0.7	0.8	1.71
20191216	0.4	0.5	–1.12

Table A12: Same as A9, but for GA.

Date	MEI	CPC ONI	Daily AO Index
20021224	0.8	1.1	–0.73
20030319	0.6	0.4	0.45
20030425	0	0	–2.07
20050322	0.8	0.4	–0.72
20060102	–0.7	–0.8	–0.61
20060113	–0.7	–0.8	1.47
20060407	–0.8	–0.3	–2.37
20070301	–0.1	0	0.11
20080315	–1.6	–1.2	–0.97
20080510	–1	–0.8	–1.19
20080511	–1	–0.8	–1.02
20090218	–0.9	–0.7	–0.7
20090410	–0.7	–2.0	0.66
20110427	–1.9	–0.6	0.7
20120302	–0.6	–0.5	1.14
20160223	1.8	2.2	–0.76
20170121	–0.2	–0.3	0.93
20170122	–0.2	–0.3	0.32
20170403	–0.4	0.3	1.68
20170405	–0.4	0.3	0.38
20190303	0.7	0.8	2.38

Table A13: Day 1 Types of Boundaries associated with TOR events 1200 UTC (%).

TOR Boundary	Stationary %	Warm %	Cold %	Other %
AL	43.8	18.8	18.8	21.9
MS	42.6	17.0	25.5	14.9
LA	37.5	29.2	16.7	16.7
GA	38.1	33.3	4.8	23.8

Table A14: Same as A13, but for NULL.

NULL Boundary	Stationary %	Warm %	Cold %	Other %
AL	36.9	9.2	15.4	38.5
MS	35.9	8.7	27.2	28.3
LA	28.6	10.2	33.7	27.6
GA	34.4	12.5	28.1	25.0

Table A15: Number of Day-1 multi-state quasi-stationary boundaries associated with TOR events 0000 UTC.

Multi-State Quasi-Stationary Boundaries	# of Events
AL–GA	21
MS–AL	25
LA–MS	12

REFERENCES

Adams-Faught, B., 2010: Dixie Alley winter tornadoes and the El Nino/La Nina teleconnection 1950–2007, Dept. of Geoscience, M.S. thesis, University of Arkansas, 114 pp.

Anderson-Frey, A. K., Y. P. Richardson, A. R. Dean, R. L. Thompson, and B. T. Smith, 2016: Investigation of near-storm environments for tornado events and warnings. *Wea. Forecasting*, **31**, 1771–1790.

——, ——, ——, ——, and ——, 2019: Characteristics of tornado events in the southeastern United States. *Wea. Forecasting*, **34**, 1017–1034.

Armstrong, H., 1953: Forecasting tornadoes in Georgia. *Mon. Wea. Rev.*, **81**, 290–298.

Brooks, H. E., Doswell, C.A. III and M. P. Kay, 2003: Climatological estimates of local daily tornado probability for the United States. *Wea. Forecasting*, **18**, 626–640.

Brown, M. C., and C. J. Nowotarski, 2020: Southeastern U.S. tornado outbreak likelihood using daily climate indices. *J. Climate*, **33**, 3229–3252.

Broyles, J. C., and K. C. Crosbie, 2004: Evidence of smaller tornado alleys across the United States based on long track F3–F5 tornado climatology study from 1880–2003. Preprints, *22nd Conf. on Severe Local Storms*, Amer. Meteor. Soc., Hyannis MA. [Available online at: http://www.spc.noaa.gov/publications/broyles/longtrak.pdf].

Bryant, B, C. Woodrum, T. A. Murphy, T. M. Stetzer, L. Walker, and T. Fricker, 2022: Analysis of the 12 April 2020 northern Louisiana tornadic QLCS. *J. Oper. Meteor.*, **10**, 43–62.

Bunker, R. C., A. E. Cohen, J. A. Hart, A. E. Gerard, K. E. Klockow-McClain, and D. P. Nowicki, 2019: Examination of the predictability of nocturnal tornado events in the southeastern United States. *Wea. Forecasting*, **34**, 467–479.

Crawford, M. E., 1950: A synoptic study of instability lines. *Bull. Amer. Meteor. Soc.*, **31**, 351–357.

Dixon, P. G., A. E. Mercer, J. Choi, and J. S. Allen, 2011: Tornado risk analysis: Is Dixie Alley an extension of Tornado Alley? *Bull. Amer. Meteor. Soc.*, **92**, 433–441.

Fulks, J. R., 1951: The instability line. *Compendium of Meteorology*, T. F. Malone, Ed., Amer. Meteor. Soc., 647–655.

Gaffin, D. M., and S. S. Parker, 2006: Climatology of synoptic conditions associated with significant tornadoes across the southern Appalachian region. *Wea. Forecasting*, **21**, 735–751.

Gagan, J. P., Gerard, A., and J. Gordon, 2010: A historical and statistical comparison of Tornado Alley to Dixie Alley. *Nat. Wea. Dig.*, **34**, 145–156.

Galway, J. G., and A. D. Pearson, 1981: Winter tornado outbreaks. *Mon. Wea. Rev.*, **109**, 1072–1080.

Gensini, V. A., and W. S. Ashley, 2011: Climatology of potentially severe convective environments from North American Regional Reanalysis. *Electronic J. Severe Storms Meteor.*, **6** (8), 1–40.

Hagemeyer, B. C., 1997: Peninsular Florida tornado events. *Wea. Forecasting*, **12**, 399–427.

——, 2010: The 2009–10 El Niño and Florida dry season tornadoes: A reality check for the limits of predictability. NOAA Climate Prediction S&T Dig., 9–14. [Available online at https://repository.library.noaa.gov/view/noaa/9379/noaa_9379_DS1.pdf.]

——, and G. K. Schmocker, 1991: Characteristics of east-central Florida tornado environments. *Wea. Forecasting*, **6**, 499–514.

Kelly, D. L., J. T. Schaefer, R. P. McNulty, C. A. Doswell III, and R. F. Abbey, 1978: An augmented tornado climatology. *Mon. Wea. Rev.*, **106**, 1172–1183.

King, P. W. S., M. J. Leduc, D. M. L. Sills, N. R. Donaldson, D. R. Hudak, P. Joe, and B. P. Murphy, 2003: Lake breezes in southern Ontario and their relation to tornado climatology. *Wea. Forecasting*, **18**, 795–807.

Kis, A. K., and J. M. Straka, 2009: Nocturnal tornado climatology. *Wea. Forecasting*, **25**, 545–561.

Klepatzki, J. P., and S. M. Milrad, 2020: Multiscale environmental analysis of cool-season Florida tornado and null events. *Electronic J. Severe Storms Meteor.*, **15** (1), 1–34.

Lee, S.-K., R. Atlas, D. Enfield, C. Wang, and H. Liu, 2013: Is there an optimal ENSO pattern that enhances large-scale atmospheric processes conducive to tornado outbreaks in the United States? *J. Climate*, **26**, 1626–1642.

——, A. T. Wittenberg, D. B. Enfield, S. J. Weaver, C. Wang, and R. Atlas, 2016: US regional tornado outbreaks and their links to spring ENSO phases and North Atlantic SST variability. *Environ. Res. Lett.*, **11**, 044008.

Lloyd, J. R., 1942: The development and trajectories of tornadoes. *Mon. Wea. Rev.*, **70**, 65–75.

Means, L., L., J. E. Hovde, W. B. Chappell, and J. M. Porter, 1955: A synoptic study on the formation of squall lines in the north central United States. *Bull. Amer. Meteor. Soc.*, **36**, 390–396.

Megnia, R. W., T. W. Humphrey, and J. A. Rackley, 2019: The historic 2 April 2017 Louisiana tornado outbreak. *J. Oper. Meteor.*, **7**, 27–39.

Mesinger, F., and Coauthors, 2006: North American regional reanalysis. *Bull. Amer. Meteor. Soc.*, **87**, 343–360.

Molina, M. J., and J. T. Allen, 2019: On the moisture of tornadic thunderstorms. *J. Climate*, **32**, 4321–4346.

——, R. P. Timmer, and J. T. Allen, 2016: Importance of the Gulf of Mexico as a climate river for U.S. severe thunderstorm activity. *Geophys. Res. Lett.*, **43**, 12295–12304.

——, Allen, J. T., and V. A. Gensini, 2018: The Gulf of Mexico and ENSO influence on subseasonal and seasonal CONUS winter tornado variability. *J. Appl. Meteor. Climatol.*, **57**, 2439–2463.

Netherton, K., and J. M. Lanicci, 2024: A climatological study of cold season tornadoes along the north central Gulf Coast. Proc., *31st Conf. on Severe Local Storms,* Virginia Beach, VA, Amer. Meteor. Soc., 131.

Porter, J. M., L. L. Means, J. E., Hovde, and W. B. Chappell 1955: A synoptic study on the formation of squall lines in the north central United States. *Bull. Amer. Meteor. Soc.*, **36**, 390–396.

Schaefer, J. T., D. L. Kelly, and R. F. Abbey Jr., 1980: Tornado track characteristics and hazard probabilities. *J. Wind Eng.*, **1**, 95–109.

Sherburn, K. D., and M. D. Parker, 2014: Climatology and ingredients of significant severe convection in high-shear, low-CAPE environments. *Wea. Forecasting*, **29**, 854–877.

——, ——, J. R. King, and G. M. Lackmann, 2016: Composite environments of severe and nonsevere high-shear, low-CAPE convective events. *Wea. Forecasting*, **31**, 1899–1927.

Skaggs, R. H., 1967: On the association between tornadoes and 500-mb indicators of jet streams. *Mon. Wea. Rev.*, **95**, 107–110.

Showalter, A., K., and J. R. Fulks 1942: Preliminary report on tornadoes, U. S. Weather Bureau, Washington, DC, 162 pp.

Stakely, A. H., 1957: A procedure for forecasting tornadoes in Alabama, Georgia, and South Carolina. *Mon. Wea. Rev.*, **85**, 151–158.

Thompson, R. L., B. T. Smith, P. T. Marsh, and A. R. Dean, 2013: Spatial distributions of tornadic near-storm environments by convective mode. *Electronic J. Severe Storms Meteor.*, **8** (5), 1–22.

Uccellini, L. W., and D. R. Johnson, 1979: The coupling of upper and lower tropospheric jet streaks and implications for the development of severe convective storms. *Mon. Wea. Rev.*, **107**, 682–703.

C. Wang, 2007: Variability of the Caribbean low-level jet and its relations to climate. *Climate*. *Dyn*., **29**, 411–422.

Wasula, A. C., L. F. Bosart, R. Schneider, S. J. Weiss, R. H. Johns, G. S. Manikin, and P. Welsh, 2007: Mesoscale aspects of the rapid intensification of a tornadic convective line across central Florida, 22–23 February 1998. *Wea. Forecasting*, **22**, 223–243.

Weaver, S. J., S. Baxter, and A. Kumar 2012: Climatic role of North American low-level jets on U.S. regional tornado activity. *J. Climate*, **25**, 6666–6683.

Williams, B. M., J. S. Allen, and J. W. Zeitler, 2018: Anticipating QLCS tornadogenesis: The three-ingredient method during the 19–20 February 2017 south-central Texas tornadic QLCS event. *Proc., 98th Amer. Meteor. Soc. Ann. Meeting*, Austin, TX, 1–22 [Available online at https://ams.confex.com/ams/98Annual/webprogram/Paper331351.html.]

REVIEWER COMMENTS

[Authors' responses in *blue italics.*]

REVIEWER A (John M. Lanicci):

Initial Review:

Recommendation: Accept with major revisions.

General Comments: This paper is an extension of the authors' 2020 climatological study that investigated cold/non-tropical-season tornadoes in Florida. This study uses the same criteria as the 2020 study for defining a tornado event and covers the same time of year (Dec–May), except this study extends into the southeastern states (LA, MS, AL, GA), using the term "Dixie Alley" as a geographic reference. The following are general comments pertaining to the paper, followed by specific, in-line comments.

The term "Dixie Alley" is not fully agreed-upon regarding which states or parts of states should be included. If the authors are going to use this term, they should at least cite a few papers that describe the various geographic interpretations of where it's located, versus. simply stating the term in the first few lines of the introduction. One suggestion would be to use the Gagan et. al. (2010) paper in the *National Weather Digest* entitled "A Historical and Statistical Comparison of 'Tornado Alley' to 'Dixie Alley'," that they already cited. This paper provides some background on the term itself in the beginning before going on to contrast Dixie Alley with the other popular but similarly not agreed-upon term "Tornado Alley."

We thank you for this suggestion. We decided to add a few sentences including references that included Gagan et al. (2010) to strengthen our introduction.

Their definition of "tornado event", which was carried over from the 2020 Florida study, is $\geq$4 tornadoes within a 24-h period. At the beginning of section 2 they mention that this criterion allows for the collection of a large enough case repository to develop composite analyses. However, the fact that it is carried over from the Florida study and is being applied to a region with a different tornado climatology than Florida should also be discussed at the beginning of section 2. In the 2020 study, the authors put their choice of >4 tornadoes in a 24-h period in the context of the climatological study from Hagemeyer (1997) that used $\geq$4 tornadoes in a 4-h period as a criterion for an outbreak on the peninsula. Here, the authors' selection of a 24-h period allowed them to gather a large enough sample to develop their composite analyses, and they used this as a definition of an *event* instead of an outbreak. Hagemeyer (1997) used the term outbreak in his study (several reviewers of the 2020 study suggested the authors consider changing from the term outbreak to something else, which the authors subsequently did). While the authors' definition of event was suitable for the Florida study, it may or may not be extensible to the rest of the Southeast, a geographic region that experiences larger outbreaks with more significant tornadoes than does most of Florida. I don't necessarily want the authors to present an exhaustive literature review of the various definitions for "outbreak" that have been presented in the past, but to provide more justification for keeping the same criteria as they used in the Florida study.

We agree adding exhaustive literature would not help in this case. We chose to add a few sentences to help argue our stance at the beginning of Section 2. Yes, the term "outbreak" varies a bit over the decades. However, applying a uniform definition may build consistency in future work.

One of the unique aspects of this climatological study is the state-by-state development of meteorological composites for tornadoes and null events. There is a potentially interesting linkage here between the timeframes for states that are "upstream" of each other, especially given the authors' creation of precursor composites at t – 48 h and t – 24 h from the event, and the fact that their database included overlapping case days among several states. However, there does not seem to be a logical explanation for starting with Alabama, then moving to Mississippi, Louisiana, and ending with Georgia. It might make more logical sense to take these analyses in geographic order by moving from west to east, which would be Louisiana,

Mississippi, Alabama, and Georgia. I would ask the authors to consider the idea of progressing in geographic order, and whether this would allow for a more logical discussion of the atmospheric features in their composites. Given the use of null case-day composite analyses for each state, there may be a reason why the authors chose the order they did. At a minimum, this choice of order should be explained by the authors in the revision.

We agree that the geographic order should be adjusted to allow a more logical discussion. Therefore, we made the suggested change to start with Louisiana and end with Georgia.

Specific comments follow. These are divided into Content and Editorial. For the sake of brevity, the Content comments can be included in the public-facing review, while the Editorial ones can be excluded.

[Editor's Note: For the published review, we keep scientifically substantive "Content" comments and omit minor ones, such as requests for reconciling references, rewording for clarity, or verbiage deletion that does not affect the substantive results.]

Content: The percentage of manufactured/mobile homes shown on the maps of Figure 1 is interesting, but I'm not sure how necessary it is, considering that this is the only place in the paper where the authors mention it. Unless you are going to expand upon this topic later in the paper, I'm not sure it needs to be presented this way.

The map was deemed necessary to emphasize vulnerability to tornado impacts. Butler (2017) and Muncy (2021) argued that well-developed areas typically witnessed higher tornado intensities.

I had a difficult time following the discussion of spatial distribution of tornado reports in the four states. How did you stratify the data to get the quartiles? It seemed as if the data assignments were arbitrary, but I could be missing something here. It should be elaborated upon and perhaps the results would be better presented in a table or even a figure.

The locations specified in the text were the overall average based on the locations of the total reports from each state. Then using the locations of those reports, we calculated the respective quartiles of from north to south. It's an attempt to show a geographic climatology where tornadoes develop during the average higher-end events.

The trough in the Null cases also appears to be located farther east than in the TOR cases at all three times.

We appreciate the reviewer for noticing that. Thus, we decided to add it to the manuscript.

[Minor comments omitted...]

Second Review:

Recommendation: Accept with minor revision.

General Comments: The following are general comments pertaining to the revised paper, followed by specific, in-line comments.

1. The authors have adequately addressed my concerns about use of the term "Dixie Alley."

2. The authors have adequately addressed my concerns about the definition of "tornado event", which was carried over from the 2020 Florida study. There will always be a degree of arbitrariness associated with defining what constitutes a tornado event as well as what a "null" event should be. The idea that this definition could allow for some uniformity across study regions appears to be reasonable.

3. The authors reordered their state-by-state review of the synoptic-scale composite analyses to one based on geography. This makes the revision clearer, especially in terms of making state-by-state comparisons.

Now that this major change has been made, there is one more aspect of this part of the study that needs to be addressed. A number of the case days are shared among one or more states. For example, LA and MS share 12 case days in this set. This suggests that the resulting composites are not completely independent of one other and influences the total counts of ENSO and AO phases since the same case days are being counted multiple times. I'm not suggesting a drawn-out reanalysis, but it should be pointed out in the final version of the manuscript so that the reader is aware that shared case days will influence the results, especially if the shared days are more common amongst adjacent states than non-adjacent states. This last point is important because the authors make extensive use of state-to-state comparisons throughout the paper.

4. There are several places in the revision where the explanations can be made clearer. It is easier to point these out in the individual Content comments [below], and I ask the authors to clarify these statements to improve readability. Additionally, there are places where "indefinite antecedents" appear. I put the term in quotes because I'm not using it in the classic sense. For example, when the preceding sentence makes multiple points, and the next sentence uses "this", it's not clear which of the points from the preceding sentence "this" is referring to. I'll also put these in the Content comments.

Specific comments follow. These are divided into Content and Editorial. For the sake of brevity, the Content comments can be included in the public-facing review, while the Editorial ones can be excluded. *[See previous Editor's Note.]*

Content: The discussion of CDC SVI data still seems somewhat out of place. Your previous sentence mentions "proximity of densely populated areas", and this could easily be illustrated with an underlay of population density in Figure 1 instead of mobile-home percentage. I think you're trying to relate the tornado occurrences to location of vulnerable populations, so suggest either replacing "densely populated areas" with "socially vulnerable population areas" or keep the text and use another measure to underlay the tornado frequencies in Fig. 1.

We decided to replace "densely populated areas" with "socially vulnerable population areas" to reflect the importance of TOR and NULL impacts across Dixie Alley.

The reference to Kelly et al. (1978) is confusing. You never actually mention which time period has the maximum occurrence frequency.

Thank you for pointing this out to us. We made an adjustment to the sentence at question to better represent Kelly's distribution of tornadoes study within the manuscript.

In the Molina et al. studies, are you referring to the SST over the Gulf?

We see the discrepancy that led to the confusion. So, we made the correction to the manuscript.

Please elaborate on how you determined the surface boundary and type. Was it based on temporal proximity to the first report of a case day? How did you handle multiple boundary types in an area?

We analyzed 1200 UTC WPC frontal boundaries to determine the type of boundary. If the first tornado report occurred after 1800 UTC but no later than 0300 UTC, we used the 0000 UTC front and determined if it persisted since 1200 UTC or longer (i.e. previous 24–48 h). This is due to some large events (e.g. 26 and 27 April 2011) that occurred over multiple days. The first tornado report must have occurred along or near the stationary boundary and no other boundary (i.e. cold, outflow, squall, or warm). If a tornado report occurred near or along the warm front, we analyzed the winds on either side to determine if they were offsetting (i.e. directional). If they were offsetting, this was an indication of possible errors within the WPC algorithm to detect fronts since offsetting winds when less than 10 kt would dictate a stationary or near-stationary front. If there were no offsetting winds and/or exceeded 10 kt of wind, it was deemed a warm front since LLJs are known to exist within the warm sector. If multiple fronts existed, the nearest front to the reports were determined to what developed the event.

I can follow the description of how you arrived at the geographic center point for each state's tornado distribution. However, the quartile description is not as straightforward. Did you stratify these west-east and south-north to arrive at these coordinates? Might be helpful to provide a short explanation.

The statistical analysis of Q3 and Q1 was made automatically upon the successful load of tornado reports within the QGIS query. Essentially, 75% of tornado reports occurred above this location for Q3 or 25% of tornado reports occurred above this location for Q1.

Either I don't agree with your interpretation of the trough evolution in Fig. 2, or perhaps it needs to be refined. I do see a notable change between –48 and –24 h, but not that much between –24 and 00 h.

We added "when the most intensification occurs" to the sentence to provide a better description of the synoptic evolution. Essentially, the pattern between –24 and 00 h exhibited persistence with a slight weakening. This will contribute to the relationship study between AO and the synoptic evolution.

There are a lot more studies that examined jet stream locations and tornado occurrences than these two (Beebe and Bates 1955; Clark et al. 2009 are two additional examples). You may want to add additional historical references here.

We appreciate the additional references and added them to the list.

I'm not sure I follow your interpretation [in that] I don't think the TOR and NULL composites are that different over LA in terms of "meridional vs. zonal" pattern. Here again, I think it's a matter of phrasing. The TOR troughs are deeper than the NULL troughs and the locations of the axes are different. There are great differences in the wind fields where the jets appear to be more spread out and less distinct in the NULL cases than the TOR cases. Here again, I think it might be advantageous to try and draw axes or at least label where you think the cores are located in the figure.

After reading the paragraph in question, we agree with your interpretation. We added "PFJ" and "STJ" labels to the jet-stream figures. Furthermore, we added another paragraph describing the TOR and NULL trough evolutions.

I'm not sure I agree with your interpretation of the trough orientation in Figs. 6–7 compared to Figs. 2–3. If you're comparing the tilt of the troughs in the LA and MS composites, the MS troughs are perhaps tilted *slightly* more negatively than the LA composites, but the MS mean troughs themselves don't have a negative tilt. You may be trying to squeeze more out of these comparisons than is possible, or perhaps a rephrasing is in order. The other possibility is that the mean MS trough at 00 h is actually composed of two shorter-wave troughs over TX that are influencing the overall composite. This happened in a study that my student did of Mobile and Baldwin County tornadoes using 20 y of event data, where we also used NARR to generate synoptic composites. When we looked at individual case days (we only had 13 of them) we could see the influence that different trough locations had on the overall composite. This seems to be evident in the 00-h MS 500-hPa composite, where you could make an argument for separate trough axes over western and eastern TX. In fact, that eastern trough could actually have a slight negative tilt.

We want to thank you for pointing this out to us! After careful review of the MS 200-hPa composite, we noticed the same thing. Therefore, we have edited the text to describe the two shortwaves across TX influencing the main trough compared to the single trough seen across LA.

Another possibility is that the TOR case convection "used up" the moisture compared to the NULL cases. A lot of these explanations are speculative at best.

Not necessarily. The gradient between the Atlantic ridge and the eastward progression of the low seen in Figures 13b,c would likely cause the increase and reduction of the PWTR. This is evident given NW LA experienced PWTR values decrease from 4–8 to 00 mm over a 24-h period with rich 8–12-mm PWTR values across SE LA through AL.

Are you suggesting that the GA mean trough has become negatively tilted by 00 h? I definitely see this in the AL data but not in the GA data, unless (as in MS) the mean trough may be capturing components that result in two shorter wave troughs: a western one over central OK to northern TX, and a second, slightly negatively tilted trough from S IL into W TN.

We are not suggesting the GA mean trough has become negatively tilted. We are suggesting the trough becomes weaker after a post AL event given a similar PFJ. GA shares a similar TOR climatology to FL but shares dynamic properties with AL.

As I mentioned previously, including an SVI underlay in the tornado frequency charts provides a loose association between severe weather and societal vulnerability. But again, I'm not sure how pertinent this is, since this is primarily a climatological study.

It is important to show the impacts of TOR and NULL cases based on the areas that are hit, [and] those most susceptible to high damage. Housing (i.e. brick or wood) does damage; however, the impacts [to] mobile homes are more life threatening.

Another suggestion for a future study would be to take this type of composite-based climatology and develop component pattern types using either a subjective or objective approach. There are a number of reliable statistical techniques for doing this, or perhaps a ML algorithm could be explored for this purpose.

We agree this could be an interesting angle to take in future work and have added a sentence at the end of the paper that mentions it.

See Netherton and Lanicci (2024) for an example of the type of geographically narrow study using very similar analysis techniques (NARR-generated composites). This work was presented at the 31st SLS and 24th Student Conferences.

Thank you for pointing us to this interesting extended abstract. We have added the reference and cited it near the beginning of Section 4.

[Minor comments omitted...]

REVIEWER B (Anthony W. Lyza):

Initial Review:

Recommendation: Decline.

Summary: This is a poorly written manuscript, where many of the claims made by the authors are simply not supported by evidence. It's unclear to me whether any of the findings, even those supported by evidence, reveal anything novel that advances severe storm prediction. Given the number of major comments, the unlikelihood that two months will be sufficient to address them all, and doubts that I have that addressing all the major comments alone will lead to a study with novel results, I recommend rejection.

Fatal Flaws: While it's clear that the authors' claim that all hits in this study were enhanced-risk events or better can't be true (see major comments below), if it were, I don't think using the 5% tornado probability contour without 4 or more tornadoes being confirmed would constitute a relevant null dataset. The null dataset should be as similar to the primary event dataset as possible. For instance, the null dataset to an event dataset where all events had a 10% or greater tornado probability contour and observed 4 or more tornadoes would be all cases were there was a 10% or greater tornado probability contour and fewer than 4 tornadoes were observed. If the null dataset is instead defined as all cases with a 5% or greater tornado probability and fewer than 4 tornadoes, to what degree do the events with a 5% max tornado probability and fewer than 4 tornadoes skew the development of the null dataset? How are those cases analogous to

the "hit" dataset? What is the ultimate meaningfulness of the results? This statistical mismatch between the event dataset and how the null dataset was developed is a fatal flaw in the methods for this study.

As we state in the manuscript, the methodology is a follow up of previous research (Klepatzki and Milrad 2020). This consistency nullifies the mismatch the reviewer mentioned as the research continues to create a larger dataset of synoptic comparisons.

The authors claim repeatedly in this study that tornado forecasting is "difficult" or "needs improvement." However, they also claim that their dataset with cases of 4 or more observed tornadoes were exclusively forecasted as enhanced risks or better. These statements are incongruent. If all their events are forecasted as enhanced risks or better, then we must be doing a pretty good job at forecasting when a tornado event is likely to occur.

We have decided to remove all mention of forecasting problems associated with tornadoes from the manuscript.

Major Comments: General comment: As a community, we need to move away from referring to the Southeast as "Dixie Alley." The term Dixie has specific historical and racial connotations we shouldn't be propagating. Instances "Dixie Alley" and "DA" should be revised to the Southeast or "SE."

We point the reviewer to Dixon et al. (2011) and Gagan et al. (2010) as relatively recent papers that use the term "Dixie Alley" in their title. [Maybe] the term should be sunset, but we don't particularly see any evidence that it has been sunset. We will default to the editor's recommendation on this issue.

[EDITOR'S NOTE: Since multiple formally peer-reviewed papers since 2000 use this term, we'll allow it, but with the acknowledgment that it is a potentially controversial colloquialism in some quarters. Unfortunately, concise alternatives are lacking. "Southeast" is too broad geographically (i.e., includes parts of the Carolinas, Florida and arguably Virginia and Kentucky, that are outside the typical "Dixie Alley" usage.)]

Attribution of Southeast tornado vulnerability to "proximity of densely populated urban areas" is a gross simplification of the problem. The authors must elaborate more on vulnerability due to factors such as poverty, mobile/manufactured housing stock, nighttime tornadoes, etc., and include relevant sources for that information.

We added a sentence to section 1, paragraph 1, to support our claim.

It's inappropriate to cite sources that are 70+ years old and have been refuted repeatedly (referencing the diurnal timing of tornadoes in the Southeast). Also, the background on nocturnal tornado frequency is incomplete without mention of Ashley et al. (2008).

We decided to remove the older references from paragraph 1. However, we kept them throughout the rest of the manuscript as they provide evidence, and like those written by Hagemeyer (1991; 1997; 2010), they can be used for verification and updated to accommodate other useful information. The text throughout this paper is a testament of this approach. We have added the Ashley et al. (2008) reference.

The enhanced-risk category wasn't debuted until 2015; therefore, not every event could qualify as an enhanced risk going back to 2002. Furthermore, prior to February 2006, there was no enhanced-risk-equivalent tornado probability contour (10%). Not only do the authors need to do significant work to clear up these errors, they need to also specify how many of the events met the 10% tornado probability threshold for a tornado-driven ENH risk.

The authors decided to add, "…since 2014 when enhanced risks were implemented, and moderate risk or greater from 2002–2013," to the paragraph that the reviewer mentioned.

The claim that, "This will continue to be an issue as the increase in prices contributes to local communities finding cheaper ways to live," is made with no evidence provided.

We have decided to remove this from the manuscript.

The claims made in this paragraph *[Editor's Note: A since-deleted topic]* seem pretty fantastical, and it's impossible to check the veracity of the sources for them because the authors did not include the citations in their list of references. Furthermore, this information is largely superfluous to the main point of the paper, which is the synoptic-scale pattern recognition of Southeast tornado events.

We decided to remove the terrain roughness paragraph from the manuscript.

Without knowing the relative frequency of La Nina vs. El Nino and +AO vs. –AO conditions during the study period, it's impossible to interpret the meaningfulness of any of these results.

The results we provided in this paper are intended to show the average teleconnection conditions associated with TOR and NULL events. Frequency isn't needed as our composites are the mean average location of features and anomaly strength.

"Upper-level winds" do not "become increasingly linear with time." Winds cannot be linear in the context of forcing convection to become linear. The shear vector can become more linear with time as a trough amplifies or low-level flow weakens and veers.

We decided to add the reviewer's comment regarding how the shear vector becomes more linear with time as low-level flow weakens and removed "related event once upper level winds become increasingly linear in time."

The "chances of QLCS development" being linked to a "wider exit region" is a link that is at best tenuous. QLCS development is more predicated on jet streak orientation and the resulting strength of ascent and the deep-layer wind shear vector.

We decided to change the sentence to reflect the zonal nature of the feature than the "wider exit region."

[Minor comments omitted...]

Second Review:

Recommendation: Accept with major revisions

Summary: This paper is somewhat improved from the initial submission. However, the paper is still somewhat disjointed in its organization, and many of the figures could be improved. There is also at least one major formatting issue in the document that leads to some of the text missing. I recommend further major revisions.

Major Comments: General comment: I understand the history of referencing the Southeast as "Dixie Alley." But I maintain that as a community, we need to move away from referring to the Southeast as "Dixie Alley." The term Dixie has specific historical and racial connotations we shouldn't be propagating. Further instances "Dixie Alley" and "DA" should be revised to the Southeast or "SE." The authors can acknowledge in a footnote that this region was colloquially been referred to as "Dixie Alley" in the past if they really wish to maintain that callback.

Due to the consideration and approval of the chief editor including the extensive reference support we provided for the use of the term, we will not be making any further changes to the manuscript regarding "Dixie Alley" and/or "DA".

How is there such a large range in the fraction of events that featured a stationary front?

We decided to rewrite the sentence to the following on page 2, "stationary boundaries occurred in 38–44% and 29–37% of our TOR and NULL cases, respectively." We appreciate you pointing this out to us.

What are the QGIS elat and elon functions? What values do they compute, and how do they compute them? These must be described in detail when first introduced.

We noticed our mistake. The elat and elon are the end latitude and longitude of tornado reports provided by SPC. Therefore, the correct reports are listed as slat and slon (i.e. start latitude and longitude). The statistical analysis is based on functions within QGIS. It takes in the spatial data within the query and conducts the analysis automatically. We updated the text in the manuscript to better reflect these points.

Was there any consideration for evaluating the trans-Nino index (TNI), given its link to tornado outbreak activity?

We have not heard of the trans-Nino Index (TNI), which is why it wasn't included in our original manuscript. We have added some language about it with the suggested reference included toward the end of the revised manuscript.

This [LA analysis] is an interesting observation that I think should be discussed further. Are these lower event numbers and higher null case numbers linked to Louisiana's geography? Given that tornado activity generally increases with northern extent across each state and Louisiana has much less northern extent than Mississippi, Alabama, or Georgia, it would seem plausible.

It is plausible. We would also argue that it could be the combination of the lesser northern extent of LA and the average location of the PFJ during TOR and NULL events as the primary dynamic variable(s).

[Minor comments omitted...]